Available online at www.sciencedirect.com
SCIENCE DIRECT
Tectonophysics 414 (2006) 9–38
TECTONOPHYSICS
www.elsevier.com/locate/tecto

TRANSALP—deep crustal Vibroseis and explosive seismic profiling in the Eastern Alps

Ewald Lüschen [a,*,1], Daniela Borrini [b], Helmut Gebrande [a], Bernd Lammerer [c], Karl Millahn [d], Franz Neubauer [e], Rinaldo Nicolich [f]

TRANSALP Working Group [g,h,i,j,k,l,m,n,o,p]

[a] *University of Munich, Department of Earth and Environmental Sciences, Geophysics Section, Theresienstrasse 41, D-80333 Munich, Germany*
[b] *ENI-E&P Division, Via Emilia 1, I-20097 S. Donato Milanese, Italy*
[c] *University of Munich, Department of Earth and Environmental Sciences, Geology Section, Luisenstrasse 37, D-80333 Munich, Germany*
[d] *University of Leoben, Institute of Geophysics, Franz-Josef Strasse 18, A-8700 Leoben, Austria*
[e] *University of Salzburg, Department of Geography, Geology and Mineralogy, Hellbrunner Strasse 43, A-5020 Salzburg, Austria*
[f] *University of Trieste, Department of Civil Engineering, Via Valerio 10, I-34127 Trieste, Italy*
[g] *University of Munich, Austria*
[h] *University of Leoben, Austria*
[i] *University of Salzburg, Austria*
[j] *University of Trieste, Italy*
[k] *University of Bologna, Italy*
[l] *University of Rome, Italy*
[m] *University of Milan, Italy*
[n] *ETH-Zurich, Switzerland*
[o] *GFZ Potsdam, Germany*
[p] *Company ENI-AGIP Division Milan, Italy*

Received 15 February 2005; received in revised form 10 September 2005; accepted 4 October 2005
Available online 20 December 2005

Abstract

The TRANSALP consortium, comprising institutions from Italy, Austria and Germany, carried out deep seismic reflection measurements in the Eastern Alps between Munich and Venice in 1998, 1999 and 2001. In order to complement each other in resolution and depth range, the Vibroseis technique was combined with simultaneous explosive source measurements. Additionally, passive cross-line recording provided three-dimensional control and alternative north–south sections. Profits were obtained by the combination of the three methods in sectors or depths where one method alone was less successful.

The TRANSALP sections clearly image a thin-skinned wedge of tectonic nappes at the northern Alpine front zone, unexpected graben or half-graben structures within the European basement, and, thick-skinned back-thrusting in the southern frontal zone beneath the Dolomite Mountains. A bi-vergent structure at crustal scale is directed from the Alpine axis to the external parts. The Tauern Window obviously forms the hanging wall ramp anticline above a southward dipping, deep reaching reflection pattern interpreted as a tectonic ramp along which the Penninic units of the Tauern Window have been up-thrusted.

* Corresponding author. Tel.: +49 171 3647569.
E-mail address: lueschen@geophysik.uni-muenchen.de (E. Lüschen).
[1] Present address: Huntloser Strasse 13, D-27801 Dötlingen, Germany.

0040-1951/$ - see front matter
doi:10.1016/j.tecto.2005.10.014

The upper crystalline crust appears generally transparent. The lower crust in the European domain is characterized by a 6–7 km thick laminated structure. On the Adriatic side the lower crust displays a much thicker or twofold reflective pattern. The crustal root at about 55 km depth is shifted around 50 km to the south with respect to the main Alpine crest.

Keywords: Seismic profiling; Vibroseis; Eastern alps; TRANSALP; Sub-Tauern-Ramp; Bi-vergent orogeny

1. Introduction

The TRANSALP transect in the Eastern Alps is the latest initiative of crossing mountain ranges in Europe with seismic imaging techniques. Similar previous efforts have been known from the Alpine-aged Pyrenees (ECORS Pyrenees Team, 1988), the Western and Central Alps (Roure et al., 1990; Pfiffner et al., 1997) and from the Variscan-aged Ural Mountains (Berzin et al., 1996). Deep seismic reflection images of these projects provided a new inventory of the orogenic architecture, showing deep reaching thrust zones, intercrustal wedging and crustal roots. This success motivated similar research in the Eastern Alps, whose crustal structure was only vaguely known (TRANSALP Working Group, 2001, 2002). In contrast to the Western Alps, the Eastern Alps are widely covered by cold and rigid crystalline and cover rock nappes (Austroalpine nappes, e.g., the Northern Calcareous Alps, the Greywacke zone and the Ötztal crystalline nappe) which originated from the Adriatic microplate and camouflage deeper structures. Only the Tauern Window allows a deeper look down to the Penninic ocean units of Bündnerschiefer and ophiolites and, finally, to the cover and basement of the European plate. Jurassic marbles cover Variscan granitic sills and Palaeozoic or Precambrian paragneisses and amphibolites.

A pre-experiment speculative crustal section was developed by Lammerer and Weger (1998; Fig. 1). It was inspired by only deep seismic velocity models from seismic refraction profiling in the 1970s (Miller et al., 1977; Scarascia and Cassinis, 1997), knowledge from surface geology and structures, and, ideas on indenter tectonics developed in the Western Alps (Pfiff-

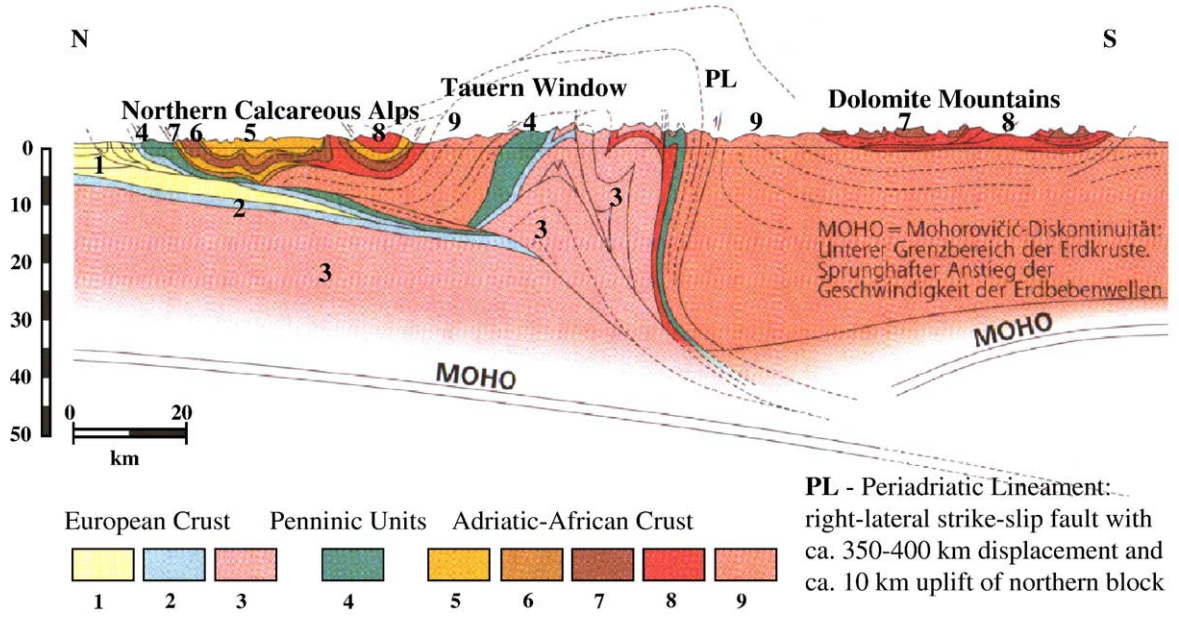

Fig. 1. Pre-experiment crustal cross-section along the TRANSALP-Traverse (modified from Lammerer and Weger, 1998). Legend: 1) Molasse sediments, folded and unfolded, 2) European Mesozoic sedimentary rocks, 3) European Variscan basement and Tauern core complex, 4) oceanic sedimentary rocks and ophiolites, 5) Upper Triassic carbonates of Adria plate, 6) Raibl beds, 7) Lower Triassic carbonates of Adriatic plate, 8) Permo-Triassic evaporates volcanics of Adria plate, porphyric granites, granodiorites, tonalities (Central Gneiss unit) in Tauern Window, 9) Austroalpine and South Alpine pre-Mesozoic metamorphic basement. Estimates of lateral and vertical displacements along the Periadriatic Lineament (PL) are in debate. Moho depths are derived from seismic refraction experiments in the 1970s (Miller et al., 1977; Scarascia and Cassinis, 1997). Adriatic crust is assumed to be more rigid than the European crust.

ner et al., 1997). Indentation of the Adriatic plate into the softer European plate was suggested to be responsible for causing the exhumation of the Penninic units exposed within the Tauern Window. The open questions addressed by the TRANSALP project were the following: Where is the boundary between the two

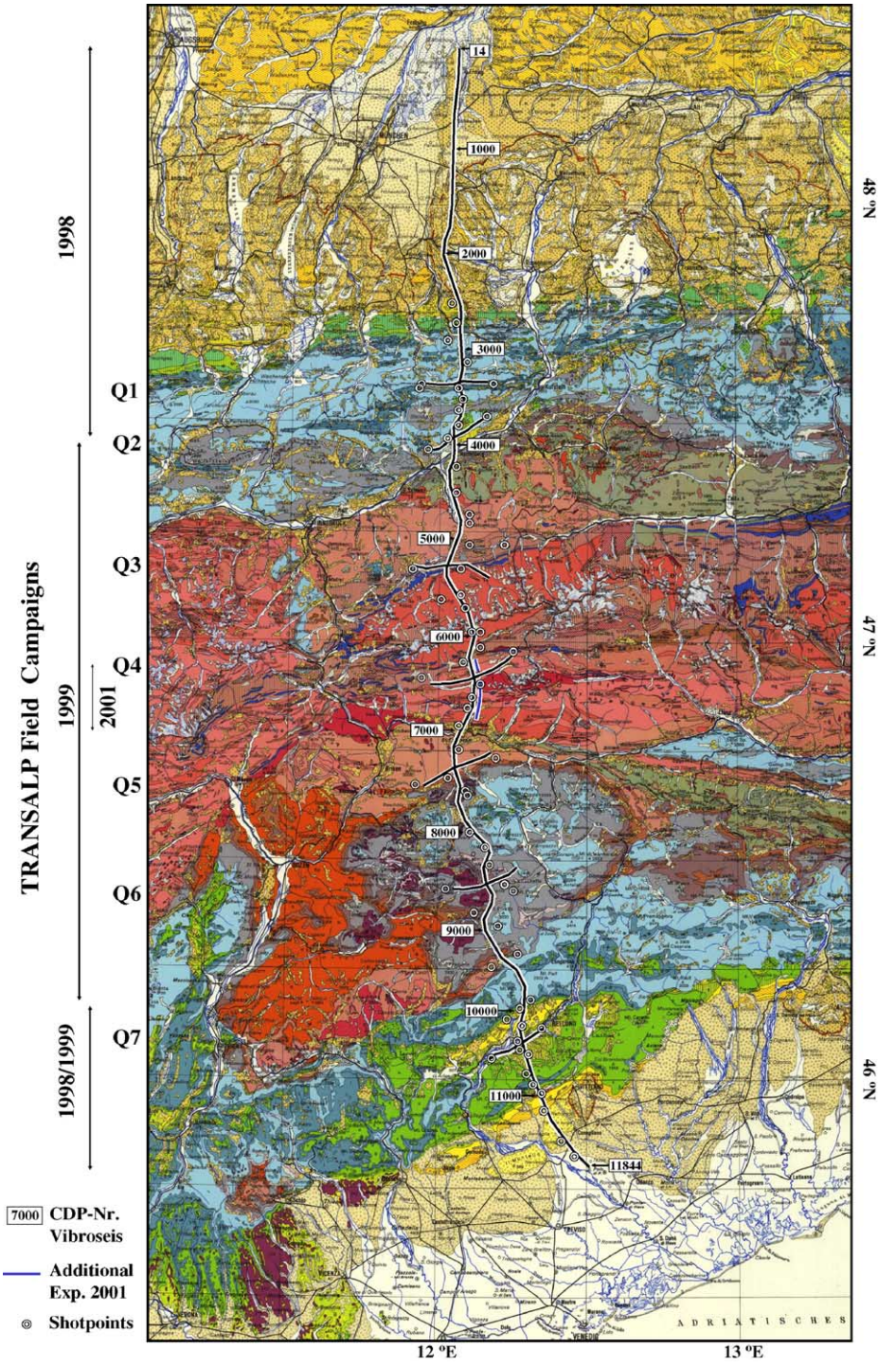

Fig. 2. Location map of the Vibroseis processing line (CMP-binning line), the cross-lines Q1–Q7 and the dynamite shotpoints, based on the geologic map of Geologische Bundesanstalt, Wien (1980), with kind permission of the director of Geologische Bundesanstalt.

Table 1
TRANSALP seismic acquisition parameters; distances in kilometers refer to line-kilometer along the receiver line (from north to south)

Vibroseis	
Length of line	340 km
Time of data acquisition	07.09.–03.10.1998 (0–120 km) 16.12.1998–29.01.1999 (290–340 km) 06.10.–22.11.1999 (120–290 km)
Contractors	THOR (0–290 km), GEOITALIA (290–340 km)
Configuration	Split spread, asymmetric in the north and south, symmetric in central sector
Length of spread	18 km (+11 km for undershooting)
Number of channels	360–361 (+220 for undershooting)
Recording instruments	1–2 ARAM 24 (0–290 km), 1 SERCEL 368 (290–340 km)
Geophone type	SM-4, 10 Hz
Number of geophones per group, group length	12 in-line, 50 m
Geophone group spacing	50 m
Seismic source	4 vibrators, electronics Pelton Advance II; Failing Y-1100 (0–120 km, total Peak Force 500 kN); Mertz M12 (290–340 km, total Peak Force 524 kN); Mertz M12 HEMI48L (120–290 km, total Peak Force 872 kN)
Source pattern	40–70 m, linear
Source point spacing	100 m (nominal)
Sweep: type, frequencies, length	Linear upsweep, 10–48 Hz, 28 s (0–290 km); 8–60 Hz, 30 s (290–340 km)
Vertical stacking	8, diversity stack (0–290 km), 12 (290–340 km)
Correlated/uncorrelated record length	20/48 s (0–290 km), 18/48 s (290–340 km)
Sampling interval	4 ms
Storage	Cartridge 3480+Exabyte 8500 (SEG-D), correlated+uncorrelated
Nominal CMP coverage	90
Explosives (if different from above)	
Length of line	280 km (starting at Vibroseis line-km 60)
Number of shotpoints on main line	47
Contractors	THOR +GEOTEC (230 km), GEOITALIA (50 km)
Configuration	Off-end, reversed
Length of spread	20–50 km, variable
Number of channels	Max. 1145
Seismic source	Dynamite in 3 drillholes
Size of explosive charge per shot	90 kg
Number of drillholes per shot	3 (nominal)
Depth of drillholes	30 m (nominal)
Tamping by	Bentonite, cement
Spacing of shotpoints	5 km (nominal)
Record length	64 s, 20 s (290–340 km)
Time break	Trigger by radio transmission via relay stations or by GPS signal, or manually by DCF77 time signal
Nominal CMP coverage	2
Cross-line recording parameters (if different from above)	
Number of cross-lines	7 (Q1–Q7)
Length of cross-lines	20 km
Spacing of cross-lines	30–35 km
Contractors	Q1 DMT; Q2, Q5 JOANNEAUM; Q3, Q4, Q6 THOR; Q7 GEOITALIA
Recording system in slave mode or directly connected to main line spread: No of recording channels	SUMMIT 2 (Q1, Q2, Q5): 240 ch; ARAM 24 (Q3, Q4, Q6): 400 ch; SERCEL 368 (Q7): 200 ch
Geophone group spacing	40–80 m
Sources per cross-line	All vibrator points and explosive shot points on main line between tie points with adjacent cross-lines plus shot points off-end on cross-lines fired repeatedly
Nominal CMP coverage	1-fold area (for bin given by source/receiver interval)

colliding lithospheric plates located? What is its geometry? Can we find traces of the former subduction zone, and what is its polarity? How did the colliding lithospheric plates interact in the middle and lower crust? Did they cause stacking and did they create shear zones? What are the differences of the deep structure of Western and Eastern Alps?

A joint German–Austrian–Italian working group was set up in early 1998 and acquired seismic data in a corridor between Munich and Venice (Fig. 2) in the period Fall 1998 to Summer 2001. The design of the experiment integrated several sub-experiments to be conducted simultaneously in an unprecedented way: (1) A Vibroseis reflection survey formed the core of the experiment, providing high-fold seismic sections with maximum resolution in the upper and middle crust. (2) Low-fold recording of high-energy dynamite sources served for better illumination of the deeper crust, eventually of the upper mantle. (3) Seven cross-lines recording vibrator and explosive sources of the main N–S line were expected to provide three-dimensional control, but they also delivered, quite unexpectedly, additional information for the 2-D interpretation. (4) Stationary arrays of continuously recording seismographs provided P-wave velocity information (Bleibinhaus and Gebrande, 2005-this volume). (5) Long-term stationary arrays were deployed for earthquake studies

and lithospheric tomography (Lippitsch et al., 2003; Kummerow et al., 2004). Here we will report on subprojects (1) and (2), which were closely coupled together, and subproject (3) regarding certain aspects of cross-line recording. The remaining subprojects will be dealt with in companion papers (Millahn et al., 2005-this volume; Bleibinhaus and Gebrande, 2005-this volume; Kummerow et al., 2005-this volume). Financial constraints were reason to subdivide the whole experiment into three main field campaigns in 1998 and 1999 (see Table 1). Due to data gaps, additional data were acquired by explosive seismic recording and gravity measurements in summer 2001.

2. Geological setting

The Eastern Alps represent a double-vergent orogen, which was formed by the collision of the European plate in a lower tectonic position and the Adriatic microplate in an upper tectonic position. The TRANSALP section is located at the greatest width of the Eastern Alps where minimal tectonic deformation could be expected and hence the clearest seismic picture. Major tectonic units in this section include from north to south (I–VIII; numbers 1–9 correspond to Fig. 1):

(I) The stable European continental basement (3) and its Post-Variscan cover (2) are unconformably overlain after the Upper Eocene by the classical wedge-shaped peripheral foreland Molasse basin (1).
(II) The Helvetic nappe complex is a small zone of Mesozoic to Eocene cover rocks detached from the stable European plate (2).
(III) The Rhenodanubian Flysch nappe constitutes Early Cretaceous to Upper Eocene turbiditic sequences (4).
(IV) The Austroalpine nappe complex comprises a mainly Variscan basement (9) and Late Carboniferous to early Late Cretaceous cover successions (5–8). Internal and deep Austroalpine nappes were ductilely deformed and variably metamorphosed during the mid-Cretaceous, Eo-Alpine ("Austrian") orogeny, which is characterized by a basically WNW-transport of units (Ratschbacher, 1986). Its cover units were accumulated in the Northern Calcareous Alps which are still juxtaposed to the Graywacke zone, which is considered as the former basement of at least part of the NCA (9).
(V) In the central Eastern Alps and structurally below the Austroalpine nappe complex, the Tauern window exposes the Mesozoic Penninic ophiolite ("Glockner nappe") (2) and
(VI) The Venediger nappe complex (or Central Gneiss unit) (3), a basement-cover complex. The Penninic ophiolite and the Central Gneiss unit are affected by Paleogene metamorphism and nappe stacking (Kurz et al., 1998 for review) and subsequent Neogene shortening with E–W elongated structural domes. The Periadriatic fault, a major regional dextral strike-slip fault to the south of the Tauern Window is decorated with Late Eocene–Oligocene plutons (Schmid et al., 1989). It separates the Austroalpine nappe complex to the south and separates it from the
(VII) Southern Alps (or Southalpine unit) (9) with the Dolomite Mountains (7) as the most prominent feature. The Southalpine unit is a basement-cover nappe complex with basically southward vergency, which is in contrast to northward transport of the all units exposed to the north of this fault. Another distinct feature is the missing metamorphic overprint of the Southalpine unit (Frey et al., 1999).
(VIII) The Southalpine unit is thrust over the Neogene–Quaternary Venetian platform, which is a foreland basin overlying the undeformed Adriatic microplate.

The Eastern Alps in its present structure are the result of Late Eocene to Neogene collision of the stable European plate with the Austroalpine and Southalpine nappe complexes after Mid-Eocene completion of southward subduction of the Penninic ocean in between (for plate tectonic scenarios, see Stampfli and Mosar, 1999). The arrangement of these units clearly demonstrates the double-vergent nature of the orogen with initial northward accretion and accumulation of nappes, and subsequent south-ward directed, still ongoing transport. During Late Oligocene and Neogene, central sectors of the orogenic edifice were affected by strong shortening and exhumation of units exposed within the Tauern window. Shortening also created a system of ca. orogen-parallel strike-slip faults including the dextral Periadriatic fault in the south and a sinistral wrench corridor along southern margins of the Northern Calcareous Alps, which also include the Inn valley fault crossing the TRANSALP section. The effect of this fault system was the lateral extrusion of central sectors of the Eastern Alps. The system was driven by indentation of the apparently rigid Southalpine unit into weak central sectors of the Eastern Alps, the Penninic units and overlying Austroalpine

nappe complex (Ratschbacher et al., 1991 and references therein).

The effect of indentation, associated shortening, generation of the strike-slip fault systems and its possible linkage with late-stage exhumation of the Tauern window were principal reasons for selection of the TRANSALP section.

3. Data acquisition: triple-mode operation

The simultaneous application of the Vibroseis and the dynamite technique in near-vertical, deep seismic reflection surveys was known as a proven technique from experiments in the Western Alps (Pfiffner et al., 1997) and the Ural Mountains (Berzin et al., 1996). According to these experiences, sufficiently deep-reaching images could be expected, since the maximum crustal thickness is in the range of 50–60 km according to earlier refraction measurements in the Eastern Alps. Upper-mantle signals were of interest, too, if seismic energy this allowed. Because of using the same recording equipment, the combination of Vibroseis and dynamite sources turned out to be relatively economic. However, the field operation required much more effort and organisation than in one single-mode operation, since direct communication over up to 40–50 km distance in Alpine terrains was necessary in order to synchronize the different field operations. Besides economics and depth penetration, there were further reasons to favour this double-mode operation. As mentioned above, the Eastern Alps, except for the Tauern Window and adjacent belts, are mostly covered by calcareous rocks (Fig. 2). These rocks usually exhibit very high impedance (seismic velocity times density) due to relatively high seismic velocities (greater than 6 km/s at the surface). As previous experience in such an environment showed, coupling of seismic sources to the ground is difficult and often results in insufficient conversion into elastic deformation in the near-source field. Additionally, energy propagation through these rocks is of reduced efficiency. Therefore, a greater chance of complete coverage was expected with the dual mode; where one source technique had deficiencies, the other could fill the gap. Another problem, which made this experiment one of the most difficult of its kind, arose from the unusually high cultural noise due to population, traffic lines, industry and tourism. The main north–south receiver line had to be deployed along almost N–S running valleys like the Ziller Valley in Austria and the Valle di Tures in Italy, and it was heavily affected by the cultural noise. The Vibroseis source technique is inherently less sensitive to such conditions, because of the sweep correlation technique and noise-reduction algorithms (i.e. diversity stack) applied during vertical stacking. However, dynamite recording required low-noise conditions, since the charges had to be kept small due to legal regulations. For the same reason, the shots could not be fired during the night (before sunrise and after sunset). The Vibroseis technique was more flexible in this respect, but suffered under the adverse noise conditions much more than it did in other, similar projects. Under these circumstances the cross-lines as the third component in this combined triple-mode field operation turned out to be a highly efficient supplement to the 2-D investigation. Since the receivers of the cross-lines were deployed in less populated east–west running valleys, the noise conditions were much more favourable than on the main line. Their source–receiver midpoint coverage was used to construct alternative north–south running sections by defining N–S binning lines for stacking. The configuration of the cross lines, the description and interpretation of their data are subject of a companion paper (Millahn et al., 2005-this volume).

Field parameters and details are listed in Table 1. During normal Vibroseis roll-along operations, dynamite shots were fired whenever the recording spread arrived at either the north or the south off-end configuration for these shots. The spare spread, in excess of the continuously recording 360 channels, in front and in the back of the rolling spread, was included after switching to dynamite mode. Thus, up to maximum 1145 channels yielding about 50 km spread length could be recorded in reversed shot configuration. A daily progress of about 5 km was achieved, including Vibroseis recording and 2–4 dynamite shots. The Vibroseis operations could rather routinely follow the main line. An exception was the construction of a new, 50 m long road across the German/Austrian border, which was built especially for the duration of this experiment. The shot points of the explosive seismic operations, however, very often had to be displaced laterally by several kilometers because of permit and safety reasons. Since they were expected to illuminate the deeper crust, the displacement can be regarded as being of minor importance. For the same reasons, the total charge of 90 kg of many of these shot points had to be split into several smaller charges and fired successively. This procedure, although mostly compensated by vertical stacking of the single partial shots, turned out to be less efficient than firing the full dynamite charge at once. Bad shots occurred (about 25%) more often than expected, although shot-holes

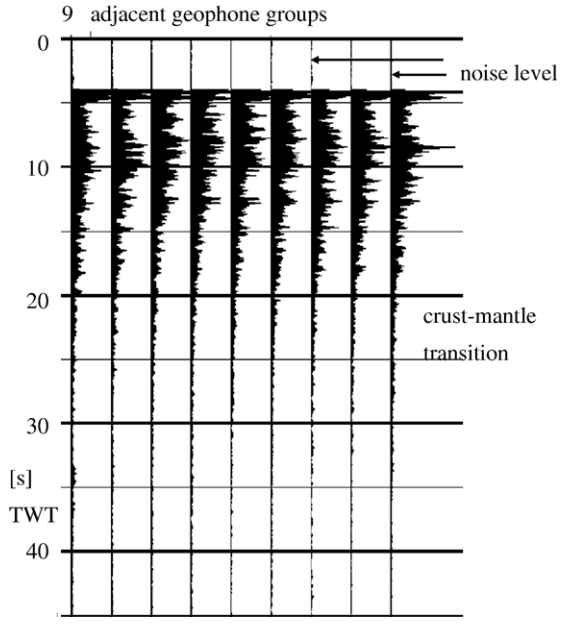

Fig. 3. Amplitude decay curves, computed from 9 typical receivers of the additional explosive experiment in 2001. Amplitude decay with time shows source energy down to 30–40 s two-way-traveltime. Traces have been extended before the ignition time to show better the typical noise level.

were carefully tamped with bentonite or cement and charges were placed below the water level. We argue that a higher amount of destruction energy is necessary in hard rock environments to create a gas volume for expansion and that hence a lower amount of energy is converted into elastic deformation in the near-source field.

In order to obtain a continuous section from the three individual field campaigns in 1998 and 1999 (Table 1), the three profile segments were combined by overlapping deployments of receivers and sources. A 6-km gap remained at the Alpine crest (Zillertal Mountains) with heights well above 3000 m. Undershooting was used to fill this gap: an additional second recording system was installed on the opposite side of the crest and operated in slave mode by radio link. The field crew handled more than 1100 receiver channels simultaneously, sometimes even up to 1500 channels, which were distributed on the main line, on two cross lines and temporarily on both sides of the Alpine crest. Synchronisation of multiple recording systems, vibrator controlling and shooting trigger boxes required radio link through several relay stations.

The northernmost (120 km) and southernmost sectors (50 km) of the line were accompanied by 250-m long shallow refraction lines for field statics computation. These were spaced about 1 km nominally and extended through Vibroseis first arrival picking. Since this approach did not achieve major improvements in comparison to statics computation from first arrival picking of the Vibroseis data only, elevation statics and subsequent residual statics, the central sector (170 km) in 1999 was done without additional shallow refraction measurements, thus saving additional costs.

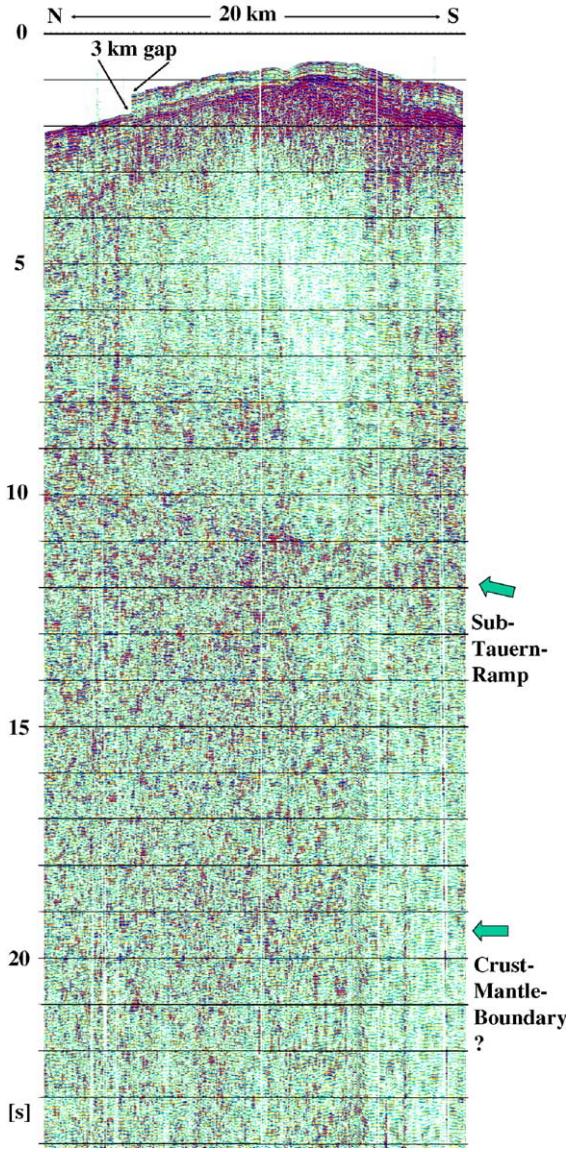

Fig. 4. Original shotgather of the experiment in 2001 after spherical amplitude correction with time and bandpass filter (8–36 Hz). Note prevailing southward dipping reflections in the middle crust at 8–12 s recording time (marked by arrow) and diffuse, but still recognisable signal energy to about 22 s in the Alpine root zone.

Table 2
Conventional Common Midpoint (CMP) processing parameters of seismic data

Vibroseis	
Data input	SEG-D format, transferred to SEG-Y in field, homogenisation by adjusting amplitude level of SERCEL records to those of ARAM records to form one consistent dataset
Crooked line geometry	24.19 m binning distance, coordinates in UTM-WGS-84 system, 3841 field-correlated records, sorting into CMP-gathers
Amplitude recovery	Spherical divergence, base $1/(t \times v^{**}2)$, gain −0.5 db/s (down to 5 s TWT)
Spike deconvolution	120 and 180 ms operator length, 2 gates, zero-phase
Bandpass filter	18–42 Hz (0–2 s), 14–40 Hz (4–20 s)
Muting	Top (for first breaks) and surgical
Automatic gain control (AGC)	400 ms (optional 1000−10000 ms)
Static correction	Elevation statics (800 m a.s.l.), velocity statics (stripping of first 2500 m according to velocity model after tomographic inversion of first breaks
NMO correction	Velocity model after continuous constant velocity stacking analysis, 50% automatic stretch mute
Residual static correction	Maximum power autostatics, smash 3, window length 8 s
Trace mixing	5 traces in CMP gather, weights 1–2–3–2–1
CMP ensemble stack	Mean stack
Bandpass filter	16−42 Hz (0−3 s), 10−36 Hz (5−20 s)
Coherency enhancement	F-x-deconvolution, horizontal window 51 traces, 7-sample operator, time window 2 s, 10−42 Hz; dip scan stack (local tau-p transform), aperture 15 traces, pass dip −10/10 ms/trace
Plot (stack section)	Cgm-plot, various scales and plot modes
Migration	Kirchhoff depth migration, multiple-arrival ray-tracing, max. dip 80°, input: stack section with bandpass, agc 2 s, f-x-deconvolution
Coherency enhancement	Dip scan stack, aperture 15 traces, pass dip −55/55 m/trace
Plot (migrated section)	Cgm-plot, various scales and plot modes
Explosive seismic data	
Crooked line geometry	50 m binning distance, coordinates given in UTM-WGS84 system, CDP 43−4684, 50 shotgathers (partly vertically stacked), bad shots omitted
Amplitude recovery	Spherical divergence, base $1/(t \times v^{**}2)$, gain −1/s (down to 6 s)
Deconvolution	Minimum phase spiking, 160 ms operator length, decon gate 500−5000 ms
Filter	Ormsby bandpass 4−8–32−44, minimum phase
Editing	Bad shots and traces
Muting	Top and surgical
Trace equalisation	Window 8000−18000 ms
Explosive seismic data	
Static correction	Final datum level: 1000 m, replacement velocity 4000 m/s, including uphole information
Normal moveout	Stacking velocity model from Vibroseis survey, stretch mute 40%
Stack	Mean stack
Pad traces	Insert missing CDP traces
Coherency enhancement	F-x-deconvolution, 51 traces horizontal window, 7 filter samples operator, time window 1000 ms, frequencies 8–32 Hz
Coherency enhancement	Dip scan stack (local tau-p transform), 15 traces aperture, dip window −16/16 ms/trace
Resample	8 ms
Migration	Kirchhoff time migration, max dip to migrate 90°, velocity model from Vibroseis survey (RMS vs time); Kirchhoff depth migration, max dip to migrate 90°, velocity model from Vibroseis survey (INTvel vs depth)
Coherency enhancement	F-x-deconvolution for time migration; dip scan stack (local tau-p transform) for depth migration, 15 traces aperture, dip window −55/55 m/trace

In order to compensate for bad shots and noise problems, as mentioned above, additional explosive measurements were conducted in the Valle di Tures south of the Alpine crest in summer 2001 (for location see Fig. 2). This time, a stationary 20-km long receiver spread was used at the eastern flank of the valley to record 4 shotpoints. It was placed about 1000 m above the previous line in a nearly noise-free environment. Amplitude decay curves (Fig. 3) show that signal energy is present up to 30–40 s recording time. Part of this energy is caused by multiply scattered and reverberated signals, which display a coda-like amplitude decay with time. However, if they occur, very deep reflections from even the upper mantle should be visible, when amplitude peaks correlate from trace to trace. Reflections from the middle and lower crust are obvious from Fig. 3. Amplitude decay curves of the Vibroseis data typically show energy down to 5–8 s, whereas the decay curves of the explosive data from 1998 and 1999 are highly variable. The shot gathered in Fig. 4 stems from the experiment in 2001, corresponding to Fig. 3, and shows a very pronounced crustal structure in the axial region of the Eastern Alps where the crustal root is expected. The uppermost crust is nearly devoid of reflections. However, a southward dipping reflection pattern is visible in the middle crust and is interpreted (see discussion below) as part of the Sub-Tauern-Ramp. Lower crustal signals occur to about 22 s (uncorrected) travel time. Explosive seismic data

have usually been recorded for 64 s. But careful inspection of these long recordings shows that no reliable signals could be obtained from depths significantly below the crust–mantle boundary.

4. Data processing

Data processing was done on different hardware and software platforms at the University of Munich, at the University of Leoben, and at the facilities of ENI-AGIP Division in Milan. Here we report on joint processing versions obtained on DISCO/FOCUS and ProMAX platforms in Munich and Leoben–partly by remote processing via Internet–and, in lesser details, on the OMEGA platform in Milan. The Milan version of the Vibroseis section has been presented at full length in the CROP Atlas (Scrocca et al., 2003). Processing details are presented in Table 2 and were first described by the TRANSALP Working Group (2001, 2002) and by Lüschen et al. (2004). Most emphasis was put on a conventional common-midpoint (CMP) stacking workflow, since it turned out to be more robust than other approaches of dip-move-out (DMO) stacking and pre-stack migration, which have been applied on selected sectors in the north and in middle of the line for comparison.

Prior to the processing, all data of the main Vibroseis line (3841 field-correlated vibratorpoint records, 27 Gb) were combined to form one consistent dataset. The data of the southernmost 50 km, recorded by a SERCEL 368 system, had to be adjusted in amplitude level due to a different instrument constant. The other data was consistently obtained by a GEOX-ARAM24 system. All coordinates of sources and receivers, originally measured in local Gauss–Krueger systems, were transferred to the UTM-WGS84 standard. The common-midpoint (CMP) numbers, also called common-depthpoint (CDP) numbers, running from 14 in the north to 11,844 in the south, and their corresponding coordinates (in meters) serve as reference for tying seismic events to geological surface structures. These CMP numbers were obtained by binning the crooked-line midpoints between sources and receivers into 25-m intervals. Strongly crooked geometry and varying recording conditions required iterative improvement of processing parameters, in particular with respect to

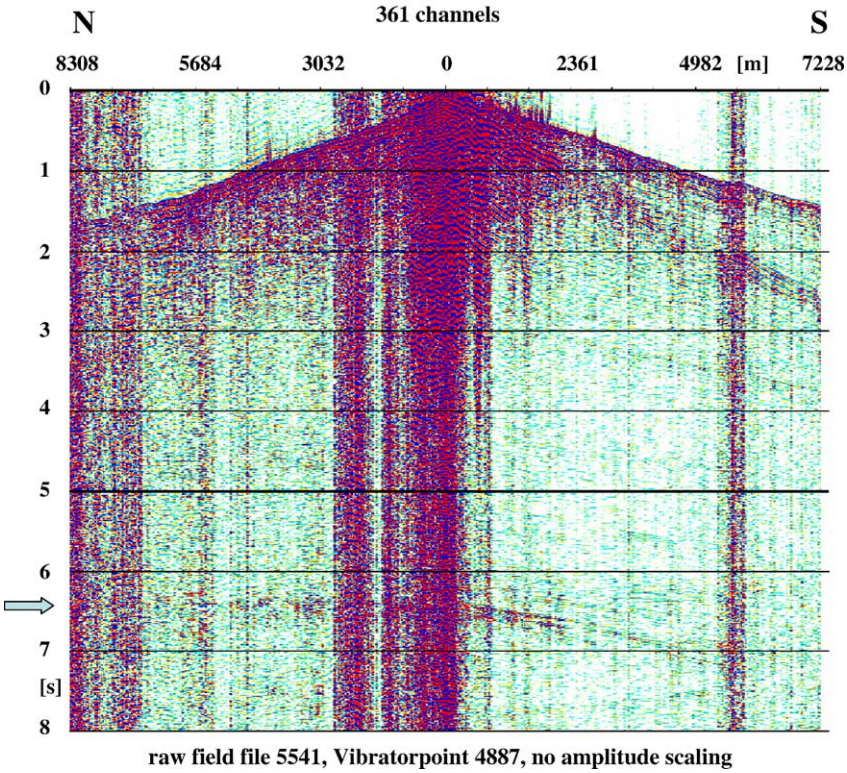

Fig. 5. Raw Vibroseis shotgather (361 channels, split spread) from south of the Tauern Window. The display shows 8 s from 20 s recorded. In this example, the number of traces distorted by traffic noise is relatively low compared to the mass of records. Note the strong reflection at about 6.5 s traveltime (ca. 20 km depth). Amplitudes are colour-coded in variable-area mode.

amplitude scaling (geometrical spreading correction and, optionally, automatic gain control AGC and trace equalisation), static correction and velocity model building. A short-window (400 ms) AGC proved to be most effective and robust for increasing the signal-to-noise ratio during stacking. Static corrections to a datum level (800 m a.m.s.l.) turned out to be a crucial step. A combination of elevation statics and velocity statics based on a tomographic inversion of the first breaks and subsequent residual statics proved to be very efficient for stacking enhancement. The complete processing history–see Table 2 for the conventional CMP processing–from geometry installation to Kirchhoff time and depth migration (post-stack) has been documented step by step for a sample portion of the line (Figs. 5 and 6).The complete line has been scanned for optimal stacking velocities by constant velocity stacking analysis (CVA) in dependence on location (CDP) and time. The velocity model required for depth and time migration was first obtained by analysis of the stacking velocities in the layered structure of the Molasse Basin areas, and secondly by tomographic inversion of the first arrivals (Fig. 7) of Vibroseis and explosive data. The latter were recorded on the main line and by the wide-aperture stationary network from Vibroseis and explosive sources. Offsets up to 80 km resulted in depth propagation to about 15 km. For the deeper part, a macro-velocity model from older, but still suitable deep seismic refraction measurements (Miller et al., 1977) was used (see discussion by Bleibinhaus and Gebrande, 2005-this volume).

A different way was chosen for the explosive seismic data (Table 2). Because of the large shotpoint interval of 5 km and the low-fold coverage, traces of best quality were selected to form a single-fold section. This was then normal-moveout (NMO) corrected, stacked on a 50 m-binning line, and finally (post-stack) time- and depth-migrated using velocity models from the Vibroseis survey. Problems occurred, as expected, due to the large shotpoint spacing and variable recording conditions, which, after low-fold stacking, did not provide a homogeneous wavefield representation suitable for the migration process. Spots of higher energy produced ‘smiles’, particularly

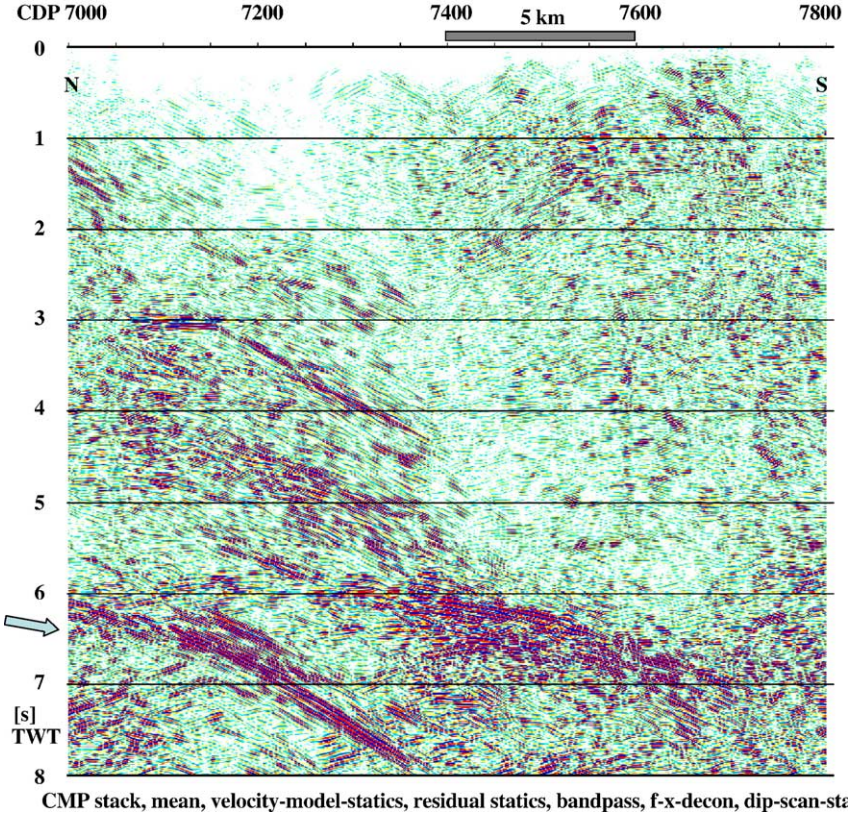

Fig. 6. Sample of the CMP stack section at a position corresponding to the shotgather of Fig. 5 (8 s shown from 20 s two-way traveltime). Amplitudes are colour-coded in variable-area mode. Arrow marks the reflection seen in Fig. 5.

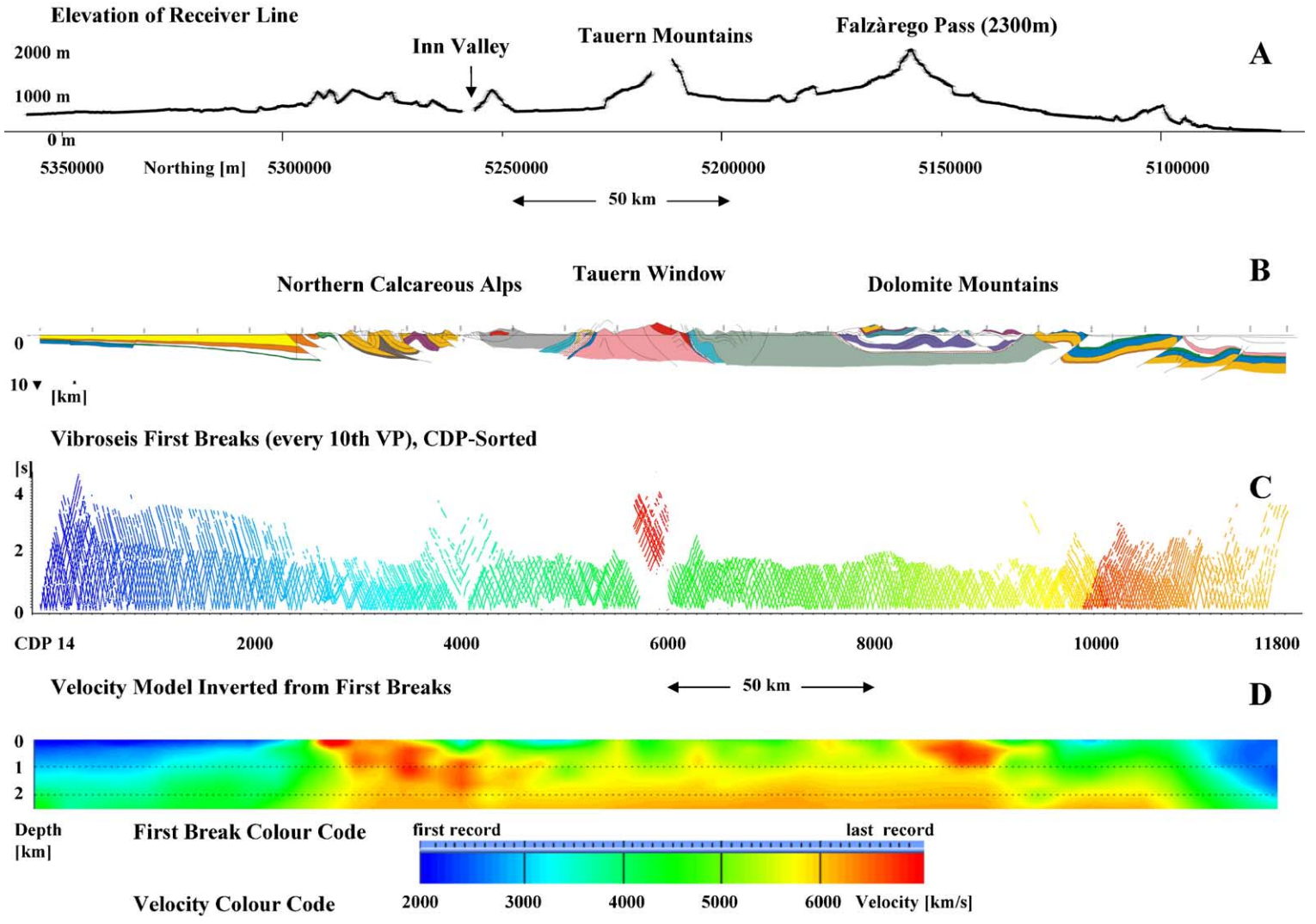

Fig. 7. Results of tomographic traveltime inversion of the first arrivals of the Vibroseis data. A: Elevation profile of receiver line. Gaps correspond to the Inn Valley and to the Tauern Mountains where undershooting deployments were chosen. B: Geological section from surface mapping and drilling information from the Molasse Basin areas. C: Traveltime–distance section of first arrivals from semi-automatic picking of every 10th shotgather. Traveltime picks are plotted over their CDPs. Colour-coding corresponds to the sequence of shotgathers in the seismic dataset. Note asymmetric split spread in the north and in the south and undershooting spreads in the Inn Valley and in the Tauern Mountains. D: Velocity model of the upper few kilometers. Note particularly high velocities in the Northern Calcareous Alps and in the Dolomite Mountains (ca. 6 km/s at the surface). Static corrections have been calculated from this velocity section.

at greater depth, which must be taken with care—as stated in a previous paper by Lüschen et al. (2004).

5. Seismic sections and interpretations

In the following chapter the seismic sections are presented, both from Vibroseis and dynamite recording. Most of them are displayed with a geological section as a header for geographical and geological orientation. The datum level of the Vibroseis sections (except Figs. 14 and 15) was set at 800 m above mean sea level.

In Fig. 6, a stack sample of the Vibroseis section south of the Periadriatic Lineament is displayed, showing strong reflections with variable and opposing dips. This is the 'cero-offset' image (in two-way-traveltime) of a bi-vergent pattern in the axial region of the Eastern Alps. During migration (Fig. 8) the individual elements of the criss-cross pattern migrate laterally over nearly 20 km in the opposite direction of their dip. The sector displayed in Fig. 8 is related to some of the most critical questions, regarding the subsurface structures of the Tauern Window and of the Periadriatic Lineament at greater depth. Two contrasting interpretations are presently discussed:

i) The reflections dipping to the south are linked to structures of the Tauern Window. In this interpretation, the Penninic Tauern units would extend far below the Dolomite mountains and cause its uplift. The Periadriatic Lineament would be confined to the Austroalpine units. It would have been cut at its base during indentation of the Southalpine block into the Tauern Window.
ii) The very strong reflections in the middle crust south of the Tauern Window are cut off along a steeply northward dipping virtual line. This line could mark the position of the Periadriatic Lineament, which, in this case should reach much deeper than in model i).

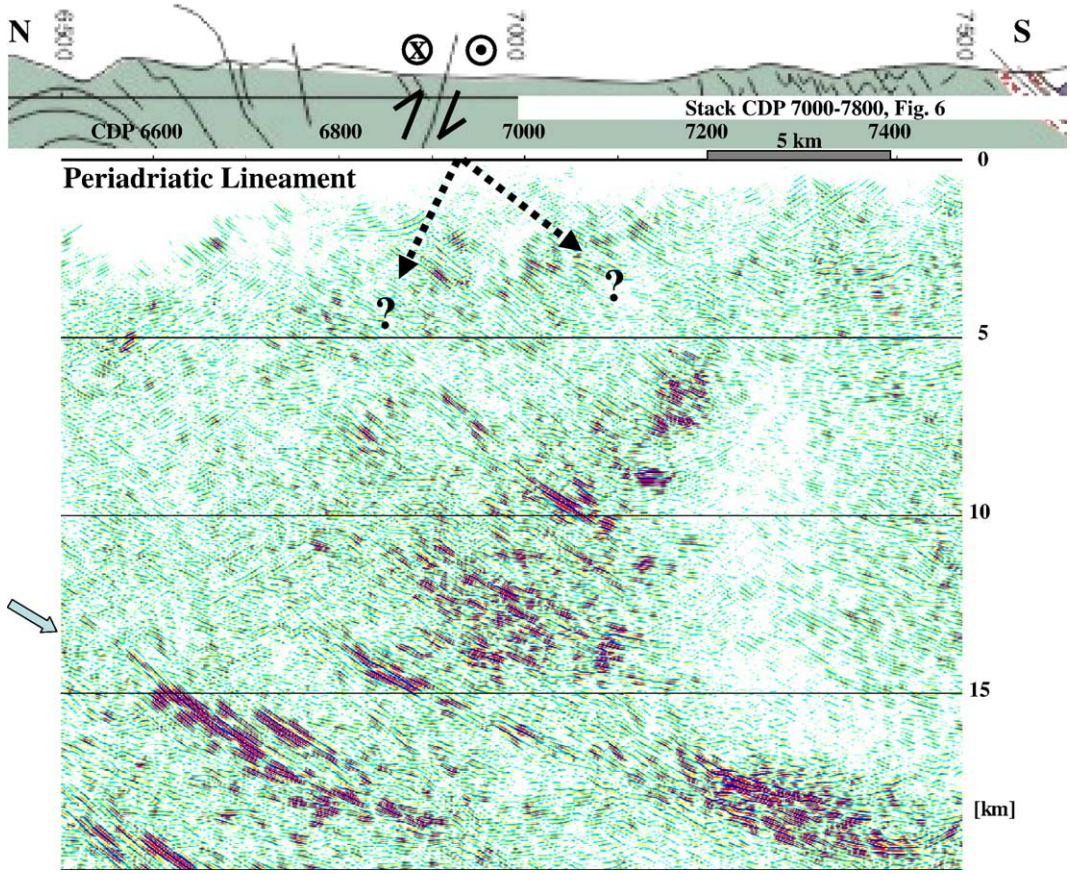

Fig. 8. Sample of the post-stack depth-migrated section, located south of the Tauern Window. The location of the stack sample (Fig. 6) is marked as a white bar for comparison. Note that the steeply southward dipping pattern in the stack section migrated about 20 km to the north. The location of the Periadriatic Lineament and its possible dip directions according to the discussion in the text is marked by arrows. The arrow on the left side marks again the reflection seen in Figs. 5 and 6.

The left dashed arrow in Fig. 8 marks the subvertical to steeply northward dipping surface outcrop of the Periadriatic Lineament (also referred to as Pustertal Fault at this location). It is considered as a major dextral strike-slip fault, which was active at around 30 to 13 Ma. Lateral displacements up to 350–400 km as well as vertical displacements of several km are discussed (e.g., Schmid et al., 1989; Mancktelow et al., 2001). We expected a considerable thickness of this zone and lower velocities because of heavy fracturing, and, to greater depth, anisotropic velocities in a ductile regime—both providing impedance contrasts for reflections. In principle, steeply dipping structures can be imaged by seismic methods, as demonstrated by Harjes et al. (1997) in case of the several hundred meter thick Mesozoic thrust fault zone of the Franconian Lineament in the Bohemian Massif. Our search for seismic reflections at the position of the Periadriatic Lineament included well-proven methods, like pre-stack migration, scanning for a wide range of stacking velocities (steeply dipping structures are often imaged using abnormal stacking velocities) and inspection of raw records for reflected diving waves. The result of all of them was negative. The conclusion might be that the fault zone is non-reflective at depth. Alternatively, if reflective, it might dip to the south corresponding to the southward dipping reflective pattern in Fig. 8 (see alternative arrow).

The nature and origin of deep seismic reflections in crystalline environments like those displayed in Fig. 8 and in almost all deep seismic profiles is extremely difficult to examine, since direct, in-situ observations are generally not possible. The difficulty is due to scattering at complex structures and inhomogenities, interference and superposition effects, and also filtering in the Earth (and in the recording system), among other causes, which distort the seismic wavelet. However, there is general consensus that the most pronounced reflections often originate at tectonic features (e.g., Harjes et al., 1997), particularly at the youngest, non-overprinted events in compressive crustal regimes. Fault zones in the upper, brittle regime are characterized by low interval velocities. In the deeper ductile regime fault zones possess anisotropic velocities, if they are mylonitized. Thus impedance contrasts necessary for creating seismic reflections can exist. Magmatic sills provide an alternative explanation. Interpretation of deep seismic reflectivity depends, therefore, on its presumed origin and the mechanical and geometrical state of the individual reflectors. Reflections from a first-order discontinuity also need a significant lateral continuity with respect to the Fresnel–Zone principles in order to be detectable, that is several kilometers at the depth of our interest. We attempted to derive some qualitative information from selected reflections of particularly high signal-to-noise ratio by comparing their signal form with that of the direct waves, which represent an approximation of the seismic source wavelet (Fig. 9). The signal

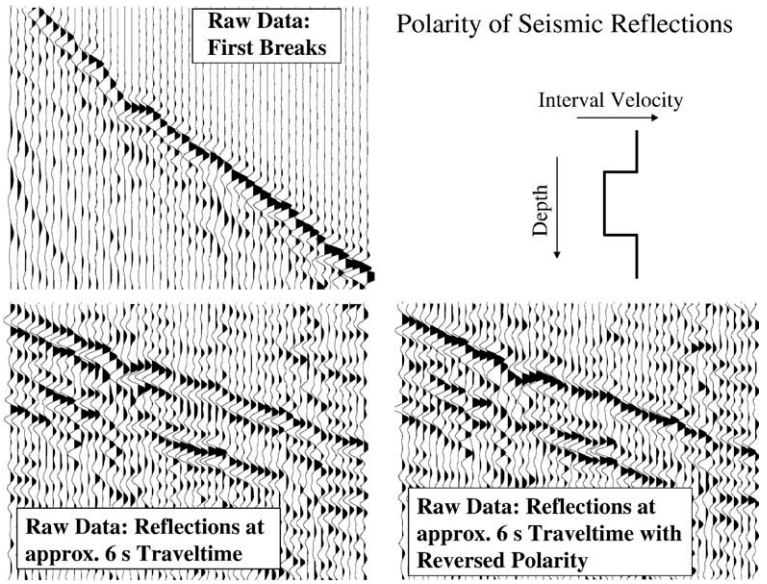

Fig. 9. Comparison of the polarity of seismic reflections with the first arrivals of the same traces within a non-processed Vibroseis record. Upper left: selected traces, 1 s long, with first arrivals. Lower left: reflections at about 6 s TWT recorded on the same traces as above, corresponding to the reflections marked in Fig. 5. Lower right: same reflections with inverted polarity. Upper right: qualitative explanation using an embedded low-velocity layer. Figure from Lüschen et al. (2004).

generally shows a maximum amplitude accompanied by two symmetrical side lobes, as typical for zero-phase Vibroseis signals. Indeed, this is approximately true for the first arrivals and the selected reflections as well; however, the sign of the reflections seems to be inverted. If the signals of the reflections are multiplied by a factor of −1, the signal form shows much better correspondence with the first arrival. This is indication that the reflection has been caused by an impedance drop (negative polarity). The opposite can be seen at a second reflection about 200 ms below. Most probably, we are therefore dealing with an approximately 500-m thick low-velocity zone embedded in a background medium with a velocity of about 6000 m/s. Since the signal form is nearly perfectly symmetric, the reflections are most likely due to first-order discontinuities rather than to interferences caused by small-scale layering. The reflection coefficient is difficult to estimate, mainly because of complex heterogeneities and interference effects. However, because of the considerable signal-to-noise ratio of the respective amplitudes, the reflection coefficient should be higher than 0.1 (Warner, 1990) and in our case negative for the upper interface. The question arises, what causes a negative impedance contrast of more than 10% at about 18–20 km depth? We favour an explanation by a tectonic origin, i.e. deformation that altered and weakened the rocks in a brittle or ductile regime, rather than by lithological–stratigraphic contrasts. Seismic velocities would then be reduced due to the creation of crack and fracture porosity, partially or totally filled by fluids (Lüschen et al., 1996). We apply this concept particularly to the extremely pronounced reflections within the bi-verging pattern south of and below the Tauern Window.

A 100 km long sector from the central part of the whole Vibroseis transect (of 300 km length) is shown in Fig. 10. At the southern flank of the Inn Valley a

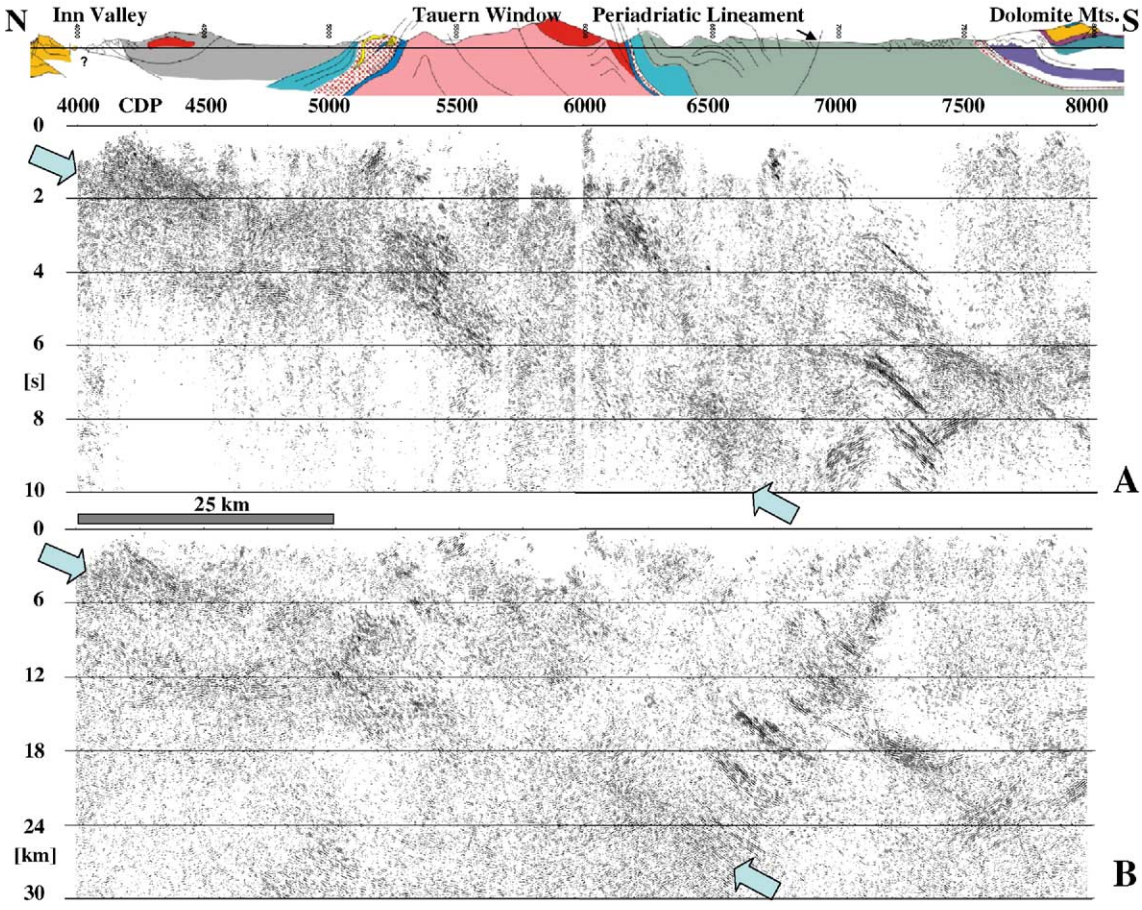

Fig. 10. Stack section (A) and depth-migrated Vibroseis section (B) between the Inn Valley and the Dolomite Mountains. Arrows mark the alignment of southward dipping reflection patterns interpreted as Sub-Tauern-Ramp, along which the Tauern Window has been upthrusted. Note

prominent south-dipping reflection pattern can be traced to the surface. This is in contrast to pre-existing ideas where north-dipping structures were expected. These reflections can be interpreted as a thrust fault system along which the Northern Calcareous Alps were over-thrusted by their former basement, the Graywacke Zone. Hereafter we interpret this structure as the outcrop of one possible branch of the 'Sub-Tauern-Ramp', which can be traced by similar reflective patterns, almost continuous, from here towards greater depth (TRANSALP Working Group, 2002; Lüschen et al., 2004). Lammerer and Weger (1998) already proposed such a ramp system, with a slightly different geometry and location, in order to explain the exhumation of the crystalline Tauern Window. The approximately 5–6 km thick pattern may consist of several slip surfaces including slices or lenses instead of a single thrust plane. Slices of Penninic units of the subducted ocean might be included within this pattern. Its internal structure is difficult to examine because of interferences, scattering and varying reflectivity characteristics. Because of its thickness at depth, the ramp system obviously does not pinch out as a single thrust system at the surface, but splits up into a larger system distributed over the whole Northern Calcareous Alps. The cover of the Tauern Window, composed of Mesozoic European sedimentary rocks, can be correlated to northward and southward dipping reflections, respectively. The internal structure of the Tauern Window at depth seems to be quite complex. However, its base is well constrained by reflection patterns characterizing the presumed Sub-Tauern-Ramp with the Tauern Window as its hanging wall. At CDP-positions 5500–6500, where the reflective character of the ramp structure is less pronounced, better images are obtained by the complementary dynamite section obtained in 2001 (Lüschen et al., 2004; compare also Fig. 4) and by alternative sections obtained from CMP-processing of the crosslines (see Millahn et al., 2005-this volume). Therefore, the reflection pattern of the presumed ramp system appears to be more continuous (to nearly 30 km depth over about 80 km distance) than visible on the section of Fig. 10 alone.

The seismic section displays an overall antiformal structure of the Tauern Window, particularly the N-dip on the northern flank of the window and the S-dip on

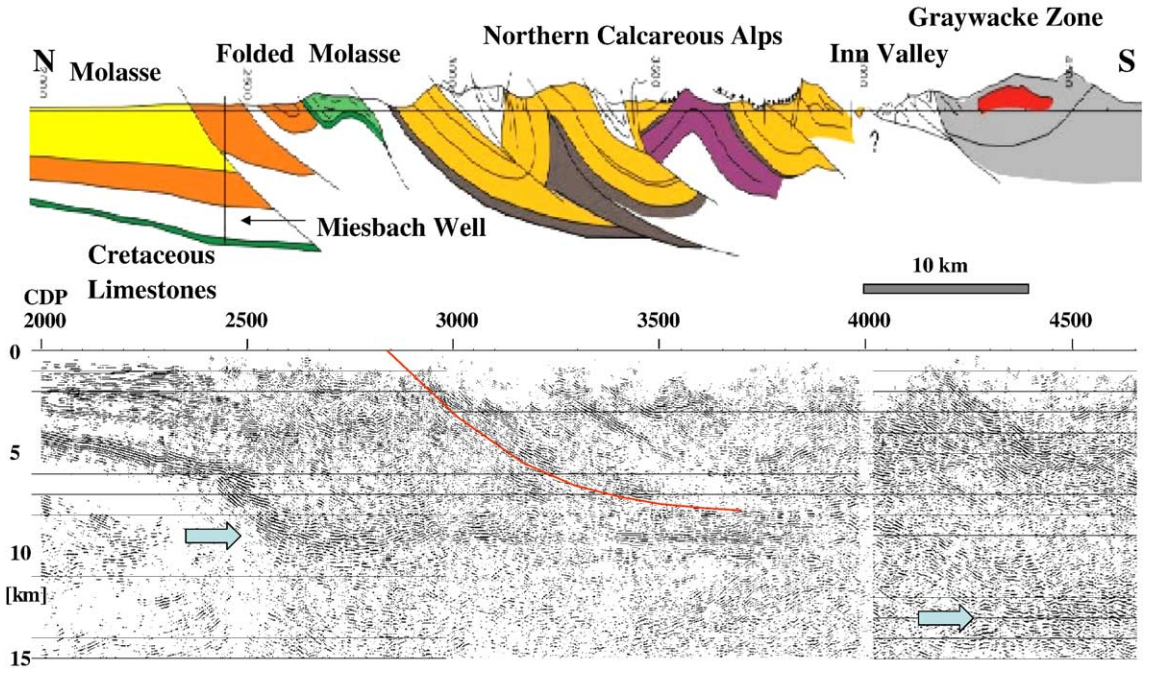

Fig. 11. Depth-migrated Vibroseis section from the Bavarian Tertiary Molasse Basin to the Northern Calcareous Alps, crossing the main Alpine front thrust system. The arrows mark displacements of the base of the Folded Molasse Basin and the Northern Calcareous Alps. The marked line denotes a transition from diffuse reflective character of the folded Molasse Basin (including Rhenodanubian Flysch and Helvetic units) to well pronounced individual southward dipping reflections of the nappes of the Northern Calcareous Alps. Velocity analysis has shown reduced velocities beneath the marked line. Well Miesbach 1 has been drilled from +709 to −5040 m (a.m.s.l.) into Lower Cretaceous limestones. Note that datum level for seismic section is 800 m a.m.s.l. Vertical scales are slightly exaggerated (ca. 1.25:1).

the southern border (Fig. 10). A crustal-scale antiformal structure forms the hanging wall above the Sub-Tauern-Ramp. Consequently, thrusting along the Sub-Tauern-Ramp contributed to exhumation of the Tauern Window and associated shortening of the up-thrusted unit. Large-scale folding of Penninic units was likely associated with a blind thrust forming a splay of the Sub-Tauern-Ramp. Such a scenario is also supported by recent analogue modelling results (Rosenberg et al., 2004), which reasonably well modelled exhumation of the Tauern Window and associated shortening by folding driven by indentation of the Southalpine unit.

Fig. 11 shows the transition from the unfolded Molasse to folded Molasse and further into the Northern Calcareous Alps. The sudden displacement by 4–5 km of the Tertiary base (top of Cretaceous limestones) and several onlap structures beneath the Alpine front little south of the Miesbach well (note arrow in left part of section in Fig. 11) were not known hitherto—despite previous industrial exploration drilling and seismic surveying in this area (Müller et al., 1988; and references therein). This could be an indication of a pre-Alpine, Mesozoic graben structure, filled by Mesozoic rocks, or of normal faulting due to the additional load of the Northern Calcareous Alps during their loading on the former European crustal basement. The folded Molasse Basin and the Rhenodanubian Flysch zones are characterized by a diffuse signature as expected, whereas the structure of the Northern Calcareous Alps seems to be well-defined with their nappes dipping to the south. At about 9–10 km depth the Northern Calcareous Alps and their substrata are bound by a basal, almost horizontal reflection pattern above a relatively transparent upper crystalline crust, similarly to the Molasse basin further north. Obviously, Mesozoic European sedimentary rocks cause this pattern, including possible tectonic slip surfaces, which were active during upthrusting of the Austroalpine calcareous and sedimentary shelf rocks of Adriatic plate origin. The marked line is correlated with the outcrop of the

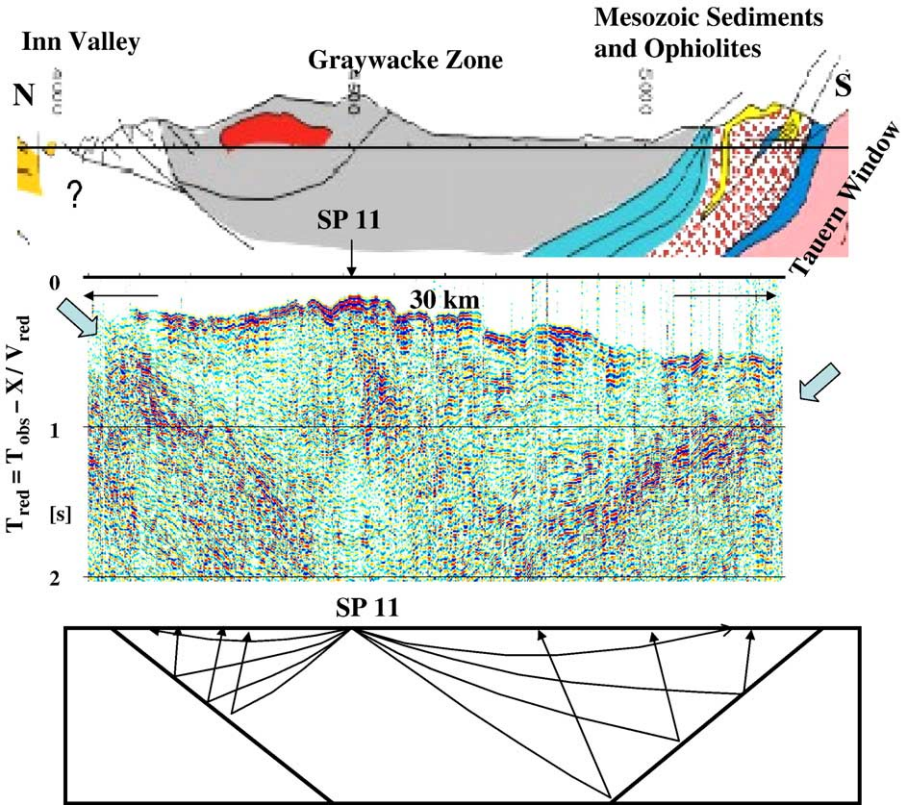

Fig. 12. Alternative representation of dipping structures, outcropping at the surface, by linear moveout display of almost unprocessed (except bandpass filters) shotgathers, in this case dynamite shotpoint 11. Time scale has been reduced by the velocity of 6 km/s. First arrivals are aligned along the horizontal distance axis, if the shallow medium is characterized by the velocity of 6 km/s. Dipping or even steep structures produce reflected diving waves which may serve as an image of these structures according to the schematic cartoon below.

basal thrust fault of the Northern Calcareous Alps and marks a transition in reflective character, from diffuse in the north to well-pronounced, individual, south-dipping reflections in the south (Fig. 11). This line limits the Northern Calcareous Alps to their substrata of Mesozoic European sedimentary rocks and to the folded Molasse and Flysch in the north. Velocity analysis for pre-stack and post-stack processing has shown that the material beneath and north of the marked line is characterized by low velocities of 4–5 km/s, underlying the Northern Calcareous Alps with velocities of 6 km/s or even higher. Therefore, we consider the possibility of hydrocarbon-bearing traps in this area, which could constitute targets for industrial exploration in the future.

Beneath the Inn Valley, there is again a throw of the sub-horizontal basement reflection pattern at the base of the Northern Calcareous Alps by about 5 km. The southward dipping reflections between these two sectors may be interpreted as part of the Alpine basal thrust in interference with the sinistral Inntal strike slip fault above. Alternatively, this pattern can be interpreted as a Mesozoic normal fault developed in the European continental margin. The basal pattern thus can be traced sub-horizontally from the Alpine front to the Tauern Window including two relatively steep displacements (see arrows in Fig. 11). The southward dipping pattern at the southern flank of the Inn Valley, as noted before, may be interpreted as an outcropping branch of the Sub-Tauern-Ramp. For detailed interpretations of the section shown in Fig. 11 the reader is referred to contributions by Behrmann and Tanner (2005-this volume) and Ortner et al. (2005-this volume).

An alternative image of steeply dipping structures, which outcrop at the surface, is presented in Fig. 12. The shotgather of dynamite shotpoint SP 11, located in the Graywacke zone south of the Inn Valley, has been displayed with a reduced time scale (or 'linear moveout'), as common for representation of crustal refraction seismic data. The first arrivals travelling with a velocity close to the reduction velocity of 6 km/s are aligned along the horizontal axis. Vertical or dipping structures produce reflected diving waves, outgoing from the first arrivals. The roof of the Tauern Window, composed of exhumed Mesozoic

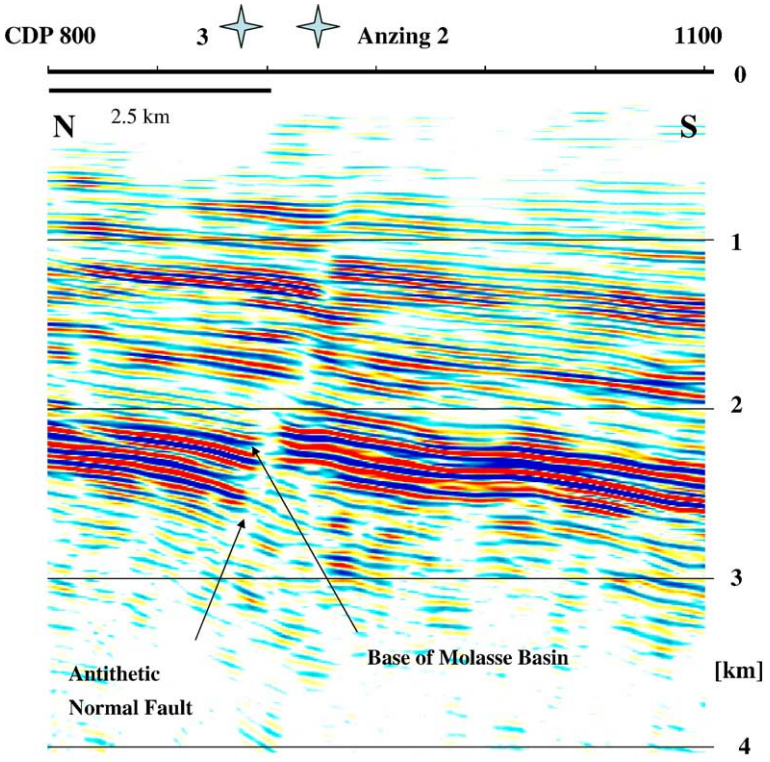

Fig. 13. Short sector of the Vibroseis depth-migrated section from the Bavarian Molasse Basin showing an antithetic normal fault, which has been a target for oil and gas exploration and production. Location of wells Anzing 2 and 3 are shown. Anzing 2, drilled into the southern block, was productive.

strata and ophiolites, is even more pronounced than in the processed sections (compare Fig. 10). During processing, such events often disappear because of muting of the wave-field along the first breaks. The whole transect has been searched for such events in this way. As mentioned earlier, with regard to such events at the Periadriatic Lineament, this search was negative.

The northernmost and southernmost parts of the 300 km long Vibroseis section display the Molasse Basins with the Tertiary base in the Bavarian Molasse and Venetian Basins as the most prominent reflection, known also from numerous industrial seismic surveying and drilling (e.g., Bachmann et al., 1982). Several former hydrocarbon exploration targets can be clearly identified at synthetic and antithetic normal faults. These faults may be due to the stretching in the outer surface of the down-bending crust. Fig. 13 displays the upper part of the Vibroseis depth-migrated section at one of these faults close to Anzing east of Munich. Thin Mesozoic sedimentary rocks and, particularly strong, the Tertiary base can be seen as subhorizontal reflections beneath the stratified Tertiary Molasse sedimentary rocks. The top of the crystalline basement is known from oil drillings nearby to be located beneath up to 600 m thick Jurassic and Cretaceous sedimentary rocks. A corresponding reflector of this surface cannot be clearly identified. Better than by depth migration is the internal structure of the sedimentary basins resolved by time migration (Figs. 14 and 15). These sections were produced at the Milan centre with special emphasis on enhancing the frequency content and resolution at shallower depths. To the south, the TRANSALP section has been prolonged by industrial sections provided by company ENI-AGIP (Fantoni et al., 2003).

Figs. 16 and 17 show a compilation of stacked and migrated sections of both, Vibroseis and explosive sources in their complete length. The Vibroseis sections are about 300 km long after the CMP-binning of the crooked line, which was originally 340 km long. The Vibroseis sections start about 90 km north of the Alpine front, whereas the explosive sections begin directly at the Alpine front. As expected, the Vibroseis sections are superior in resolution in the upper and middle crust, but show deficits in the lower crust due to the lack of signal energy. The explosive sections fill these gaps, having

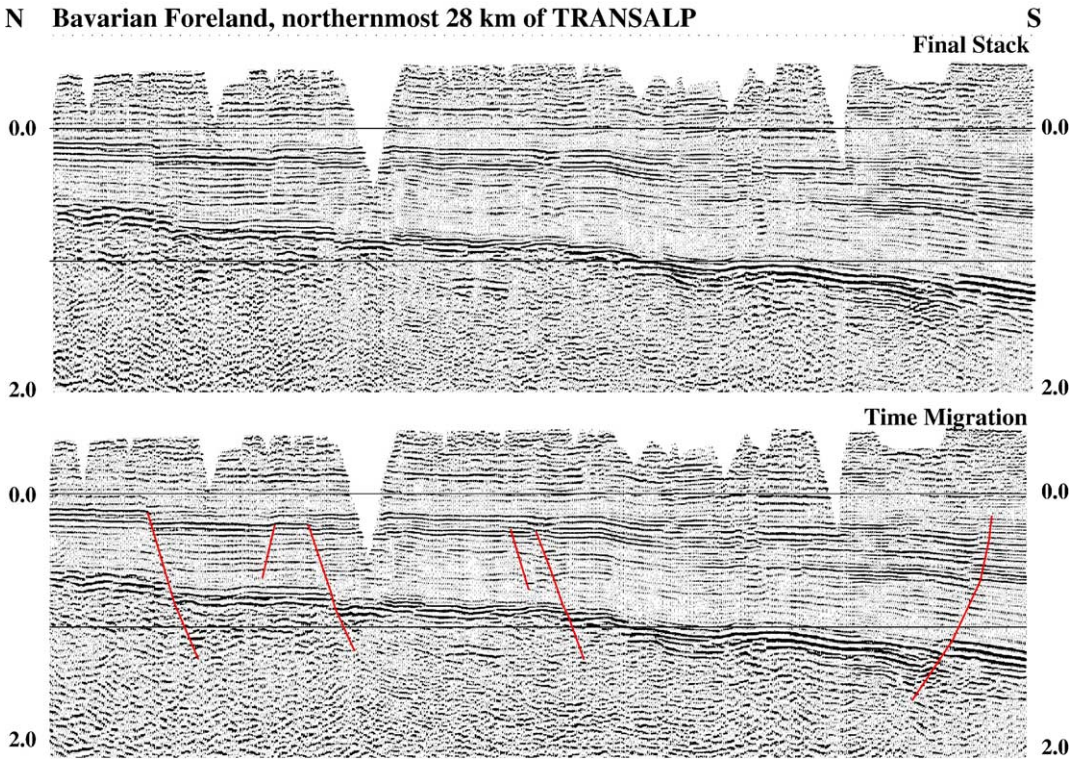

Fig. 14. Vibroseis section of the northernmost Bavarian Molasse Basin foreland after time-migration. Lower part with interpreted steep normal faults. Fault shown in Fig. 13 (Anzing) at the right side. Datum level: mean sea level.

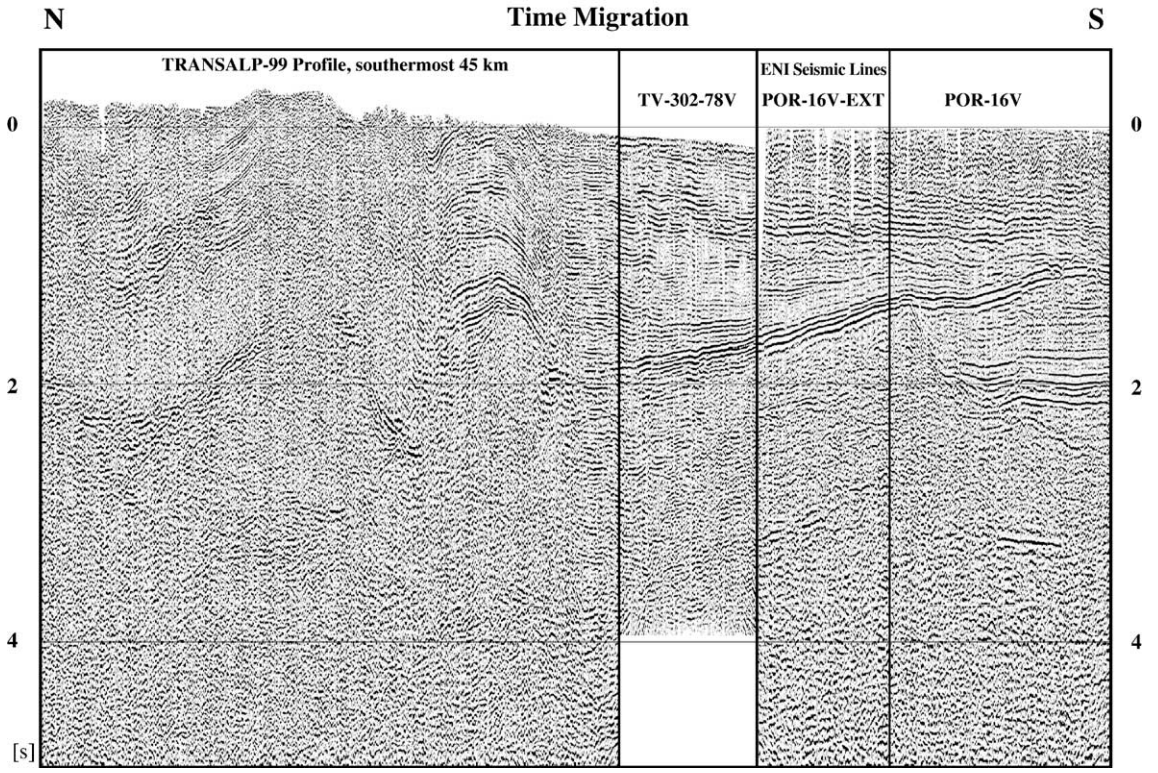

Fig. 15. Vibroseis section of the southern part of the TRANSALP transect, after time-migration (note strong vertical exaggeration), extended towards south by industrial seismic lines (courtesy of ENI-AGIP, after Fantoni et al., 2003). From left to right: Belluno synform, Montello thrust, Venetian Molasse foreland Basin with the pronounced flexure of the Mesozoic carbonate platform (see also Castellarin et al., 2005-this volume). Datum level: mean sea level.

their imaging potential mainly in the lower crust due to the experimental design. With respect to the lower crust, both methods complement each other in an optimal way. A synoptic view of stack (zero-offset time), time and depth migrated sections is necessary to evaluate these sections—because of well-known difficulties in migration of deep-crustal events. Despite these problems, which tend to produce 'smiles', both migration techniques were reasonably successful. This is, for instance, documented by the predominant criss-cross reflection pattern in the Vibroseis section of Figs. 6 and 8. After depth migration (similarly after time migration) the elements focus well and migrate to their position, as expected from the ray-theoretical point of view, and produce a bi-verging pattern. Nevertheless, lower crustal reflective spots and sectors in the Vibroseis section produce smiles because of their truncated character and smear out along the section. This effect is inherent of the migration principles, generally for deeper crustal targets in 2-D seismic surveys, and required therefore careful interpretation. It is a drawback particularly for the low-coverage explosive survey, which exhibits several spurious signals at lower crustal levels. Ray-theoretical and Fresnel-zone principles, as well as a retrospect to unprocessed field records helped to distinguish real and spurious signals.

The arrows in the line drawing of Fig. 17 separate two obviously distinct crustal domains of the section, cutting through the core of the orogen from the surface at the Inn Valley with an angle of 30° to the south over a length of about 100 km. This structure is interpreted to have acted as a tectonic ramp upthrusting the southern onto the northern block and referred as the 'Sub-Tauern-Ramp'. South-dipping sub-parallel reflections dominate the hanging wall of the ramp. Further south, prevailing northward-dipping reflections in the middle crust may be interpreted as a backthrust system and may be partly linked with the Valsugana–Agordo thrust system at the surface (further discussion by Castellarin et al., 2005-this volume). The northern block, on the contrary, is characterized by an almost transparent middle crust. It is overlain by the highly reflective and stratified Molasse Basin and by a 9–10 km thick package of the Northern Calcareous Alps, which are characterized by south-dipping reflections

and by an almost horizontal base reflection pattern. This base pattern shows two abrupt downward offsets at the Alpine front and beneath the Inn Valley. The Northern Calcareous Alps, known to be part of the Adriatic–African domain as most of the southern block except the Tauern Window, seem to be overthrusted by its former basement along the Sub-Tauern-Ramp. The northern block, except the Northern Calcareous Alps, can be viewed as European crust in collision with the Adriatic–African crust. The top of the European crystalline crust, identified by the base of Tertiary Molasse Basin and Northern Calcareous Alps, and the bottom of the crust, identified with the base of the reflective lower crust, are almost sub-parallel and show a continuous downward flexure towards south.

The section displays some remarkable asymmetries in crustal structure. The Alpine root, if taken by the lowermost reflections, with a maximum depth of 55–60 km is shifted to the south with respect to the main Alpine crest within the Tauern Window. The reflective lower crust on the European side is remarkably thinner than on the Adriatic-African side in the south. Both seem to be separated by the Sub-Tauern-Ramp. The 6–7 km thick European lower crust is also much thinner than 50 km further north of the TRANSALP transect, where previous DEKORP seismic reflection data (Meissner and Bortfeld, 1990) detected a reflective interval between 15 and 30 km depth beneath a relatively transparent upper crystalline crust. The apparent thinning of the lower crust beneath the Bavarian Molasse Basin, the Northern Calcareous Alps and the Tauern Window with respect to the adjacent northern regions remains enigmatic. Because of the bending of the European lower crust, it is clear that the generation of the lower crustal reflective structures started before the collision process of the European and Adriatic continental margins during the Alpine orogeny.

The asymmetry in the Alpine crustal structure correlates with an asymmetry in crustal velocities obtained from refraction and wide-angle seismic measurements (Bleibinhaus and Gebrande, 2005-this volume). The middle and lower crust on the Adriatic side is characterized by higher velocities than the respective European crust. The middle-lower crust on the Adriatic–African side reveals two distinct, almost sub-parallel, patterns of seismic reflections in the explosive sections (Fig. 17). This 25-km thick (or stacked?) lower crust is confirmed by corresponding velocity peaks determined by previous seismic refraction profiling. It seems to be restricted to the Southern Alps (Scarascia and Cassinis, 1997). A possible explanation has been presented by Lüschen et al. (2004), based on two-dimensional restoration of the N–S section. A lower crustal stacking in this area could be the result of tectonic erosion and accretion at depth during the subduction process.

The crustal root zone at the transition from the European to the Adriatic–African domain at 55–60 km depth is lacking reflectivity. This has been explicitly confirmed by the additional explosive experiment in 2001, which was characterized by an extremely high signal-to-noise ratio at the corresponding recording times of 15 to 20 s. Only the northern half of the 20 km long additional experiment shows lower crustal reflectivity belonging to the European crust (Lüschen et al., 2004). The asymmetry in crustal thickness and Moho geometry is also imaged by receiver functions (RF)–an imaging technique from below–obtained from teleseismic recordings of the long-term stationary network along the TRANSALP traverse, which we consider as a valuable complementary tool to reflection seismic seismology (Kummerow et al., 2004). The European Moho dips gently southward from 35 km beneath the northern foreland to a maximum depth of 55 km beneath the northern front of the Dolomite Mountains in the south in accordance with lower crustal seismic reflections (Fig. 18). However, the Moho extends nearly 20–30 km further south than visible on the reflection seismic section. This is probably due to the better capabilities of the RF to image thicker velocity gradient zones in contrast to the better resolution of the reflection seismic technique which is primarily sensitive to small-scale heterogeneities in impedance. This is obviously the case in the Adriatic part of the section, where much less correlation between RF and seismic reflections is discernable. Here the RFs show a disruption of the Moho at the northern front of the Dolomite Mountains. Because of the difference in resolution characteristics (vertical as well as horizontal, of the order of 10–100) between the two techniques, we do not want to stress the immediate Moho transition from the European to the Adriatic crust as seen by the RFs, nor inner-crustal discontinuities, a corresponding discussion is presented by Kummerow et al. (2004). The Moho geometry as derived from refraction and wide-angle modelling correlates well with the bottom of lower crustal reflectivity on the European side (compare Bleibinhaus and Gebrande, 2005-this volume). However, the Moho on the Adriatic side coincides better with the RF-derived geometry. This is indication that seismic refraction and wide-angle measurements and the RF technique are both sensitive to thick velocity

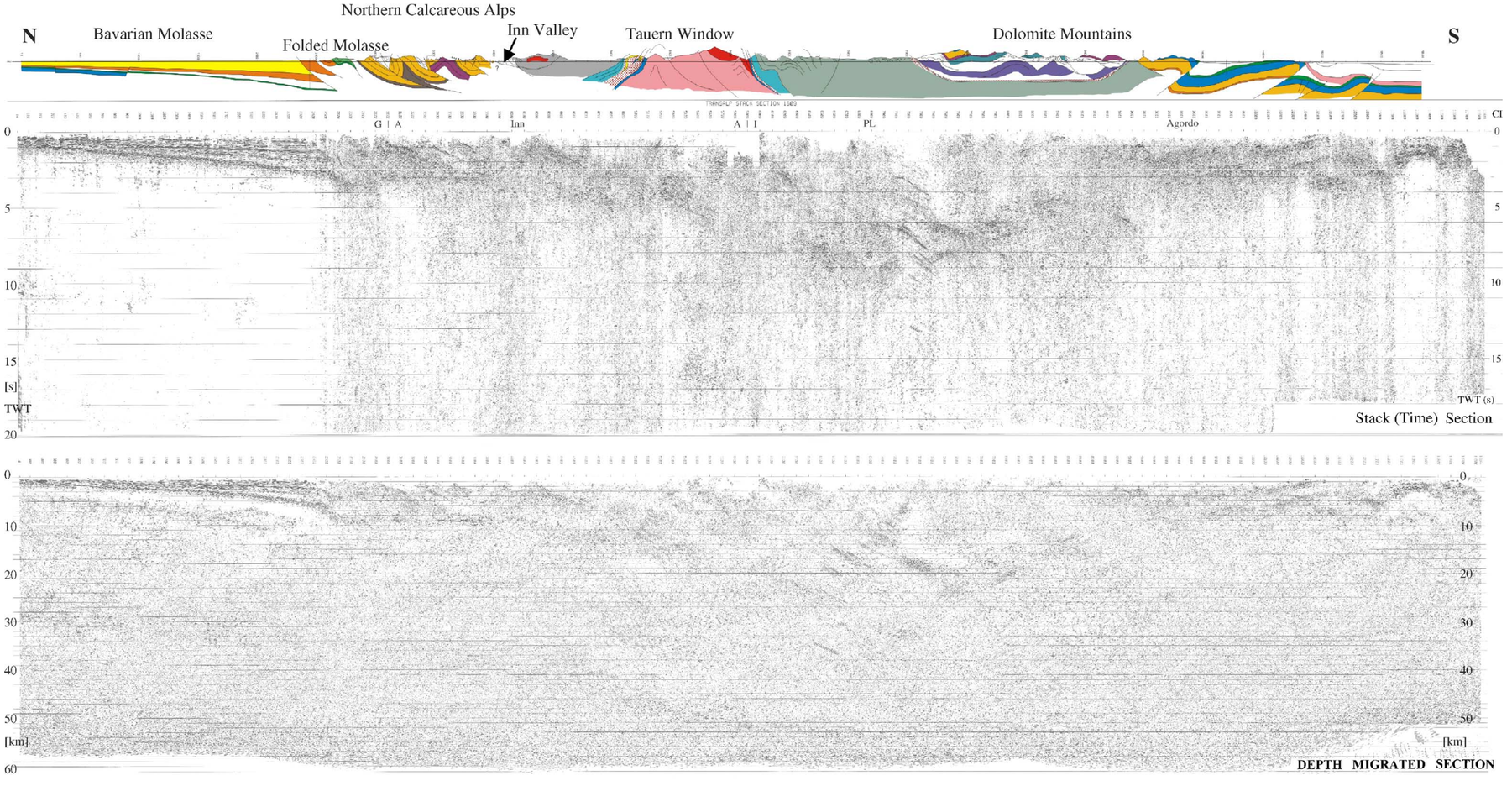

Fig. 16. Compilation of complete Vibroseis sections of the TRANSALP transect. Top: Stack section, bottom: depth-migrated section. The stack section has been produced by using a 20 s long AGC window before stacking in order to maintain relative amplitudes. A 2 s long AGC window was used for input into the migration scheme in order to make the wavefield more coherent. Scale 1 : 1, length of sections: 300 km.

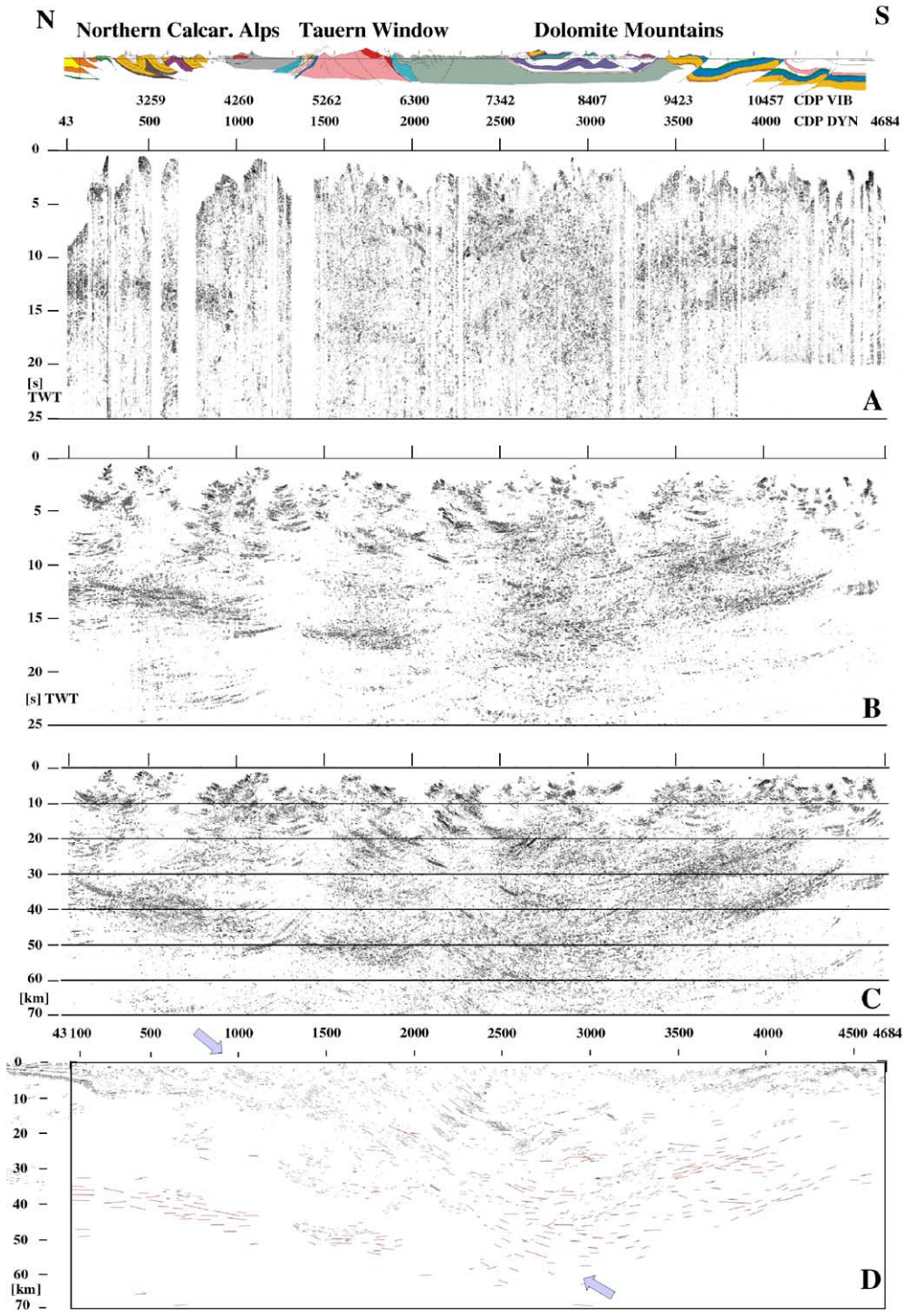

Fig. 17. Compilation of complete dynamite sections of the TRANSALP transect. The sections start in the North at the Alpine front: A: Stack section, B: time-migrated section, C: depth migrated section (with maximum migration aperture), D: compilation of manual line drawings of the Vibroseis sections (in black) and the dynamite sections (in red, emphasising mainly the lower crust). The arrows mark approximate position of the presumed thrust system of the Sub-Tauern-Ramp. (For interpretation of the references to colour in this figure legend, the reader is referred to the web version of this article.)

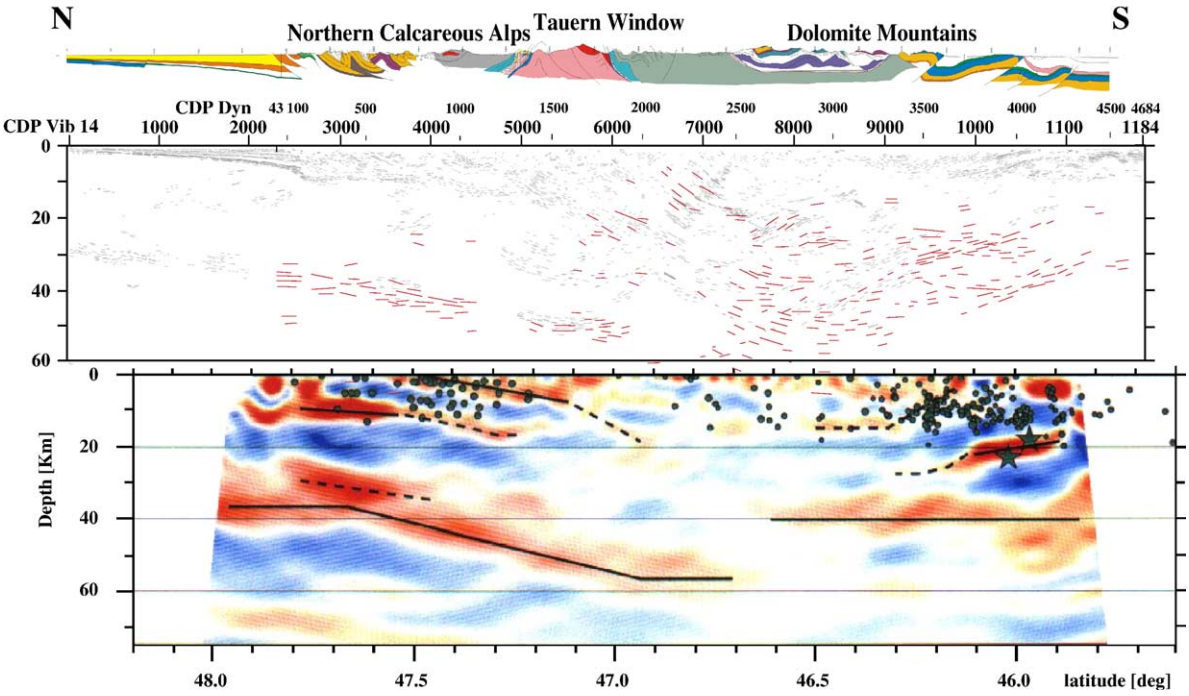

Fig. 18. Comparison of the reflection seismic section (Vibroseis reflections in black, explosive seismic reflections in red colour), represented as line drawing (top), with a depth-migrated receiver function section (bottom, modified from Kummerow et al., 2004). The maximum within the red-coloured receiver functions corresponds to the assumed P- to S-wave converting main discontinuities (black lines). Also shown here focal depths of earthquakes since 1975; stars denote particularly strong earthquakes (see discussion by Kummerow et al., 2004).

gradient zones in a similar way. Thus, the lowermost reflections on the Adriatic side in near the crustal root zone have to be considered as being originated at uppermost mantle structures and/or to lesser extent as due to side effects.

6. Conclusions

We have presented the seismic data base of the TRANSALP transect traversing the Eastern Alps between Munich and Venice. The interpretation was kept to a minimum, since the companion papers of this volume are focussed on more detailed interpretation. The key observations are the following:

(1) The Alpine axis is characterized by a bi-vergent structure at whole crustal scale.
(2) A synoptic view on Vibroseis, dynamite and cross-line sections reveals a dominant ramp-like structure: the Sub-Tauern-Ramp, dipping to the south, separating two distinct crustal domains, which differ in seismic reflection characteristics: the former European continental margin, down-bending southward, carrying the rootless, allochthonous Northern Calcareous Alps, and, secondly, the Adriatic basement with more pronounced reflectivity, having upthrusted and exhumed the Tauern Window.
(3) A crustal root at approximately 55 km depth is recorded, shifted to the south with respect to the main Alpine axis, and an asymmetric crustal structure with a thin lower reflective crust on the European side and a thick or doubled reflective lower crust on the Adriatic side.

Acknowledgements

The TRANSALP programme is jointly financed by the Bundesministerium für Bildung und Forschung (BMBF, Bonn), the Bundesministerium für Wissenschaft und Verkehr (BMWV, Vienna), the Consiglio Nazionale delle Ricerche (CNR, Rome) and the company ENI-AGIP (Milan). The TRANSALP group comprises partners from universities of Munich, Leoben, Bologna, Salzburg, Milan, Rome, Trieste, ETH-Zürich, GFZ Potsdam and company ENI-AGIP. We thank our contractors, THOR Geophysikalische Prospektion GmbH, Kiel, Germany, DMT, Essen, Germany, JOANNEUM Research, Leoben, Austria, GEOITALIA Sp.A., Milan, Italy, GEOTEC Sp.A., Campobasso, Italy, and

O.G.S., Trieste, Italy, for their excellent and enthusiastic work in difficult terrain and under difficult logistical conditions, even during winter. We appreciate administrative services provided by the GFZ Potsdam. The seismic programme is accompanied by other interdisciplinary research projects funded and coordinated by the Deutsche Forschungsgemeinschaft (DFG), Österreichischer Fonds zur Förderung der wissenschaftlichen Forschung and the Consiglio Nazionale delle Ricerche (CNR). We thank Kurt Grubbe for comments on a earlier version and Cestmir Tomek and Randell Stephenson for helpful reviews.

References

Bachmann, G.H., Dohr, G., Müller, M., 1982. Exploration in a classic thrust belt and ist foreland: Bavarian Alps, Germany. AAPG Bulletin 66, 2529–2542.

Behrmann, J.H., Tanner, D.C., 2005. Structural synthesis of the Northern Calcareous Alps, TRANSALP segment. Tectonophysics 414, 225–240. (this volume)

Berzin, R., Oncken, O., Knapp, J.H., Pérez-Estaún, A., Hismatulin, T., Yunusov, N., Lipilin, A., 1996. Orogenic evolution of the Ural Mountains: results from an integrated seismic experiment. Nature 274, 220–221.

Bleibinhaus, F., Gebrande, H., 2005. Crustal structure of the Eastern Alps along the TRANSALP profile from wide-angle seismic tomography. Tectonophysics 414, 51–69. (this volume)

Castellarin, A., Nicolich, R., Fantoni, R., Cantelli, L., Sella, M., Selli, L., 2005. Structure of the lithosphere beneath the Eastern Alps (southern sector of the TRANSALP transect). Tectonophysics 414, 259–282. (this volume)

ECORS Pyrenees Team, 1988. The ECORS deep reflection seismic survey across the Pyrenees. Nature 311, 508–511.

Fantoni, R., Della Vedova, B., Giustiniani, M., Nicolich, R., Barberi, C., 2003. Deep seismic profiles through the Venetian and Adriatic foreland (Northern Italy). TRANSALP Conference, Trieste, Extended Abstract Volume. Mem. Sci. Geol. 54, 131–134 (Padova).

Frey, M., Desmons, J., Neubauer, F., 1999. The new metamorphic maps of the Alps: introduction. Schweiz. Mineral. Petrogr. Mitt. 79, 1–4.

Geologische Bundesanstalt, 1980. Geologische Karte der Republik Österreich und der Nachbargebiete: 3. Unveränderter Nachdruck, 1:500 000, Wien.

Harjes, H.-P., Bram, K., Dürbaum, H.-J., Gebrande, H., Hirschmann, G., Janik, J., Klöckner, M., Lüschen, E., Rabbel, W., Simon, M., Thomas, R., Tormann, J., Wenzel, F., 1997. Origin and nature of crustal reflections: results from integrated seismic measurements at the KTB superdeep drilling site. J. Geophys. Res. 102, 18267–18288.

Kummerow, J., Kind, R., Oncken, O., Giese, P., Ryberg, T., Wylegalla, K., Scherbaum, F., 2004. A natural and controlled source seismic profile through the Eastern Alps: TRANSALP. Earth Planet. Sci. Lett. 225, 115–129.

Kummerow, J., Kind, R., TRANSALP Working Group, 2005. Shear wave splitting in the Eastern Alps observed at the TRANSALP network. Tectonophysics 414, 117–125. (this volume)

Kurz, W., Neubauer, F., Genser, J., Dachs, E., 1998. Alpine geodynamic evolution of passive and active continental margin sequences in the Tauern Window (eastern Alps, Austria, Italy). Geol. Rundsch. 87, 225–242.

Lammerer, B., Weger, M., 1998. Footwall uplift in an orogenic wedge: the Tauern Window in the Eastern Alps of Europe. Tectonophysics 285, 213–230.

Lippitsch, R., Kissling, E., Ansorge, J., 2003. Upper mantle structure beneath the Alpine orogen from high-resolution teleseismic tomography. J. Geophys. Res. 108, doi:10.1029/2002JB002016.

Lüschen, E., Bram, K., Söllner, W., Sobolev, S., 1996. Nature of seismic reflections and velocities from VSP-experiments and borehole measurements at the KTB deep drilling site in southeast Germany. Tectonophysics 264, 309–326.

Lüschen, E., Lammerer, B., Gebrande, H., Millahn, K., Nicolich, R., TRANSALP Working Group, 2004. Orogenic structure of the Eastern Alps, Europe, from TRANSALP deep seismic reflection profiling. Tectonophysics 388, 85–102.

Mancktelow, N.S., Stöckli, D.F., Grollimund, B., Müller, W., Fügenschuh, B., Viola, G., Seward, D., Villa, I.M., 2001. The DAV and Periadriatic fault systems in the Eastern Alps south of the Tauern Window. Int. J. Earth Sci. 90, 593–622.

Meissner, R., Bortfeld, R.K. (Eds.), 1990. DEKORP-Atlas, Results of Deutsches Kontinentales Reflexionsseismisches Programm. Springer, Berlin.

Millahn, K., Lüschen, E., Gebrande, H., TRANSALP Working Group, 2005. TRANSALP-cross-line recording during the seismic reflection transect in the Eastern Alps. Tectonophysics 414, 39–49. (this volume)

Miller, H., Gebrande, H., Schmedes, E., 1977. Ein verbessertes Strukturmodell für die Ostalpen, abgeleitet aus refraktionsseismischen Daten unter Berücksichtigung des Alpen-Längsprofils. Geol. Rundsch. 66, 289–308.

Müller, M., Nieberding, F., Wanninger, A., 1988. Tectonic style and pressure distribution at the northern margin of the Alps between Lake Constance and the River Inn. Geol. Rundsch. 77/3, 787–796.

Ortner, H., Reiter, F., Brandner, R., 2005. Kinematics of the Inntal shear zone–sub-Tauern ramp fault system and the interpretation of the TRANSALP seismic section, Eastern Alps, Austria. Tectonophysics 414, 241–258. (this volume)

Pfiffner, O.A., Lehner, P., Heitzmann, P., Mueller, St., Steck, A. (Eds.), 1997. Results of NRP20—Deep Structure of the Alps. Birkhäuser Verlag, Basel.

Ratschbacher, L., 1986. Kinematics of Austro-Alpine cover nappes: changing translation path due to transpression. Tectonophysics 125, 335–356.

Ratschbacher, L., Frisch, W., Linzer, G., Merle, O., 1991. Lateral extrusion in the Eastern Alps: Part 2. structural analysis. Tectonics 10, 257–271.

Rosenberg, C.L., Brun, J.-P., Gapais, D., 2004. Indentation model of the Eastern Alps and the origin of the Tauern Window. Geology 32, 997–1000.

Roure, F., Heitzmann, P., Polino, R. (Eds.), 1990: Deep structure of the Alps. Mém. Soc. géol. Fr.156, Paris; Mém. Soc. géol. Suisse 1, Zürich; Vol. spec. Soc. Geol. It. 1, Roma. 367 pp.

Scarascia, S., Cassinis, R., 1997. Crustal structures in the central-eastern Alpine sector: a revision of the available DSS data. Tectonophysics 271, 157–188.

Schmid, S.M., Aebli, H.R., Heller, F., Zingg, A., 1989. The role of the Periadriatic line in the tectonic evolution of the Alps. In: Coward,

G.M., Dietrich, D., Park, R.G.Alpine Tectonics. Geol. Soc. Spec. Publ., vol. 45, pp. 211–227.

Scrocca, D., Doglioni, C., Innocenti, F., Manetti, P., Mazzotti, A., Bertelli, L., Burbi, L., D'Offizi, S. (Eds.), 2003. CROP Atlas: seismic reflection profiles of the Italian crust, Descr. Carta Geol. d'Italia, vol. 62. 194 pp.

Stampfli, G.M., Mosar, J., 1999. The making and becoming of Apulia. Mem. Sci. Geol. 51, 141–154.

TRANSALP Working Group, 2001. European orogenic processes research transects the Eastern Alps. AGU, EOS Trans. 82, 453, 460–461.

TRANSALP Working Group, 2002. First deep seismic images of the Eastern Alps reveal giant crustal wedges and transcrustal ramps. Geophys. Res. Lett. 29, doi:10.1029/2002GL014911.

Warner, M., 1990. Absolute reflection coefficients from deep seismic reflections. Tectonophysics 173, 15–23.